# Erythropoietin-dependent Acquisition of CD71$^{hi}$CD105$^{hi}$ Phenotype within CD235a$^{-}$ Early Erythroid Progenitors

Natascha Schippel[1], Mrinalini Kala[2], and Shalini Sharma[1]*

[1]Department of Basic Medical Sciences, College of Medicine-Phoenix, University of Arizona, Phoenix, Arizona, USA
[2]Flow Cytometry Core, College of Medicine-Phoenix, University of Arizona, Phoenix, Arizona, USA

*Correspondence: shalinijs@arizona.edu

**Abstract**

The development of committed erythroid progenitors and their continued maturation into erythrocytes requires the cytokine erythropoietin (Epo). Here, we describe the immunophenotypic identification of a $CD34^-$ colony-forming unit-erythroid (CFU-E) progenitor subtype, termed late CFU-E (lateC), that arises in an Epo-dependent manner during human early erythropoiesis (EE). LateC cells lack CD235a (glycophorin A) but have high levels of CD71 and CD105, characterized as $Lin^-CD123^-CD235a^-CD49d^+CD117^+CD34^-CD71^{hi}CD105^{hi}$. Analysis of *ex vivo* cultures of bone marrow (BM) $CD34^+$ cells showed that acquisition of the $CD71^{hi}CD105^{hi}$ phenotype in lateC occurs through the formation of four other EE subtypes. Of these, two are $CD34^+$ burst-forming unit-erythroid (BFU-E) cells, distinguishable as $CD71^{lo}CD105^{lo}$ early BFU-E (earlyB) and $CD71^{hi}CD105^{lo}$ late BFU-E (lateB), and two are $CD34^-$ CFU-E, also distinguishable as $CD71^{lo}CD105^{lo}$ early CFU-E (earlyC) and $CD71^{hi}CD105^{lo}$ mid CFU-E (midC). The EE transitions are accompanied by a rise in CD36 expression, such that all lateC cells are $CD36^+$. Patterns of CD34, CD36, and CD71 indicate two differentiation routes—in one earlyB lose CD34 to form earlyC, and in another, earlyB gain CD36 and $CD71^{hi}$ expression prior to losing CD34 to form midC, bypassing the earlyC stage. Regardless of the route, the transition from midC to lateC requires Epo. All five EE subtypes could be prospectively detected in human BM cells and, upon isolation and reculture, exhibited the potential to continue differentiating along the erythroid trajectory. Finally, we find that all five EE populations can also be detected in cultures of cord blood-derived $CD34^+$ cells at levels similar to those observed in BM $CD34^+$ cell cultures.

## Introduction

Differentiation of hematopoietic stem cells (HSCs) to erythrocytes or red blood cells (RBCs) is dependent on erythropoietin (Epo), a cytokine produced and released by the kidneys [1-3]. Epo is necessary for the survival and continued differentiation of erythroid-lineage-committed progenitor colony-forming unit-erythroid (CFU-E) cells in both humans and mice [4,5]. Mice lacking Epo or its receptor (EpoR) die by embryonic day 13.5 due to a lack of mature RBCs [6-9]. Binding of Epo induces homodimerization of EpoR, which stimulates the receptor-associated Janus Kinase 2 to phosphorylate EpoR and itself [10,11]. This process is associated with the downstream activation of a gene expression program that inhibits apoptosis and promotes survival, proliferation, and continued differentiation of CFU-E [2,12-15].

Classically, the development of erythrocytes from HSCs has been described as a multistage process that progresses through intermediate progenitors, including multipotent progenitor (MPP) and common myeloid progenitor (CMP) [16-20]. The latter give rise to the bipotent megakaryocyte-erythroid progenitor (MEP), from which the erythroid progenitor burst-forming unit-erythroid (BFU-E) cell arises. The formation of BFU-E from MEP and their conversion to CFU-E, a phase referred to as early erythropoiesis (EE), is followed by terminal erythroid differentiation (TED). The transition of CFU-E to proerythroblast (ProEs) marks the onset of TED and is associated with the canonical erythroid lineage marker CD235a (glycophorin A). ProE develop through basophilic erythroblast (BasoE), and polychromatic erythroblast (PolyE), which finally form orthochromatic erythroblast (OrthoE). The enucleation of OrthoE forms reticulocyte, which ultimately mature into RBC.

Immunophenotyping strategies have defined transitions during human EE and TED utilizing previously established markers. These include early markers that are present in hematopoietic stem and progenitor cells (HSPCs) and persist into EE or TED, such as CD117 (c-kit) and CD49d ($\alpha$-4 integrin), transiently expressed markers, such as CD36 (fatty acid translocase), CD105 (endoglin), and CD71 (transferrin receptor), and mature markers that arise late in differentiation and persist on mature RBCs, such as CD235a and CD233 (Band 3) [21-29]. Conventionally, the BFU-E to CFU-E transition has been associated with loss of CD34, acquisition of CD36, and increased expression of CD71 and CD105, where BFU-E are characterized as $CD34^{+}CD36^{-}$ and CFU-E as $CD34^{-}CD36^{+}$ [22,23,25,30]. Notably, an intermediate $CD34^{+}CD36^{+}$ population has also been reported [21,30-32]. While some studies have found expression of CD71 and CD105 in bipotent MEPs, others have shown that CD71 and CD105 arise later, at or just before commitment to the erythroid lineage [23,25-27].

EE cells have been shown to be heterogenous and immunophenotypically resolved in both humans and mice. In prospective analysis of human BM cells, EE progenitors were resolved into four distinct subsets based on the expression of CD34 and CD105 on $CD235a^{-}CD117^{+}CD45RA^{-}CD41^{-}CD123^{-}CD71^{+}$ cells, including one BFU-E (EP1) and three CFU-E populations (EP2-4) [22]. This strategy has been widely applied and has provided valuable information on proteomic changes and effects of cytokines [33-35]. Assessment of IL-3, SCF, and Epo treatment on the four sorted EP1-EP4 populations showed lack of an effect of IL-3 on proliferation or differentiation, whereas SCF increased proliferation and decreased differentiation of all four EE populations into erythroblasts, as measured by the percentage of $CD235a^{+}$ cells [35]. Epo, however, induced a variable response in the four subpopulations. Isolated EP1 and EP2 exhibited significantly higher proliferation than EP3 and EP4, whereas EP3 and EP4 differentiated more efficiently than EP1 and EP2 in response to Epo. Importantly, lack of Epo increased cell death in EP2-EP4, suggesting that Epo not only plays a role in proliferation of EP1-EP4 but is also necessary for the survival of EP2-EP4. In another

immunophenotyping analysis, two CFU-E subtypes were resolved within the $CD34^+CD36^+$ cohort: immature CFU-E, which were, $CD34^+CD36^+CD71^{hi}CD105^{med}$, and mature CFU-E, which were $CD34^+CD36^+CD71^{hi}CD105^{hi}$ [31]. Of these two, the immature CFU-E were found to be much more responsive to SCF and dexamethasone treatment. Additionally, in a single cell mass cytometry analysis of human cord blood (CB) $CD34^+$ HSPC cultures, four CFU-E populations were detected, two of which were $CD34^-CD45RA^-CD123^-CD36^+CD71^+CD235a^-$ but differed based on CD38 positivity: CFU-E1 were $CD38^+$ and CFU-E2 were $CD38^-$ [36]. The other two, CFU-E3 and CFU-E-like, expressed the same combination of markers as CFU-E2, but at a lower level, and the CFU-E-like lacked CD36 and CD71. Studies in mice have also used CD71 and CD105, and in addition CD150, to stratify the $Lin^-Kit^+CD55^+CD49f^-CD105^+$ EE population, identifying one BFU-E subtype as $CD150^+CD71^-$ and two CFU-E subtypes based off scaled expression of CD71: early CFU-E ($CD71^{lo}CD150^+$) and late CFU-E ($CD71^{hi}CD150^+$) [37-39]. All three EE populations were observed in murine BM and spleen, however, only early CFU-E exhibited significantly increased proliferation in response to Epo treatment of mice [38].

In this study, we utilized immunophenotyping of *ex vivo* cultures of human BM $CD34^+$ HSPCs to assess the influence of Epo on heterogeneous EE population dynamics. Based on profiles of established markers, we resolved the EE compartment into five subpopulations, identifying two $CD34^+$ BFU-E, termed early BFU-E (earlyB) and late BFU-E (lateB), and three $CD34^-$ CFU-E subtypes: termed early CFU-E (earlyC), mid CFU-E (midC), and late CFU-E (lateC). These five EE populations could also be resolved prospectively in BM cells and detected during *ex vivo* differentiation of CB $CD34^+$ HSPCs. Additionally, comparison of cells undergoing differentiation in the presence and absence of Epo identified the conversion of midC to lateC, which is associated with the acquisition of the $CD71^{hi}CD105^{hi}$ immunophenotype, as the crucial Epo-dependent step. In medium lacking Epo, there was a significant decrease in the formation of lateC with a concomitant accumulation of earlyC and/or midC. Transition of earlyB to lateC was accompanied by a steady increase in CD36 expression, which, in combination with loss of CD34 and gain of CD71, identified two potential differentiation routes: one progresses through earlyC and other through lateB formation. Overall, this study resolves heterogeneity in EE cells to pinpoint the key differentiation stage which requires Epo for further development to the erythroid lineage during the differentiation of human BM and CB HSPCs.

## Results

### Epo-associated Dynamics of CD71 and CD105 Expression

To examine Epo-induced development of erythroid cells, we applied a previously established protocol for *ex vivo* differentiation of human BM-derived $CD34^+$ HSPCs [40-42]. Longitudinal immunophenotypic assessment of CD235a in cultures grown in medium containing Epo (+Epo) or lacking Epo (−Epo) revealed a robust $CD235a^+$ population in +Epo cultures but not in −Epo cultures (Figure S1A and B). Additionally, assessment of erythroblast populations using the flow cytometry strategy developed by Yan et al. showed the presence of all five erythroblast populations (ProE, early BasoE, late BasoE, PolyE, and OrthoE) in +Epo but none in −Epo cultures (Figure S1C) [22]. Examination of markers that have previously been used to distinguish and characterize EE and TED populations, including CD49d, CD117, CD36, CD71, and CD105 showed that the percentages of cells expressing CD71 (day 4), CD105 (days 4 and 7), and CD36 (days 4, 7, and 10) were significantly reduced in −Epo cultures, while those expressing CD49d and CD117 were unaffected (Figure 1A and D, and Figure S2) [16,22-25,27,43]. CD71 and CD105 exhibited low and high expression levels during the course of differentiation (Figure 1B and E). Notably, the $CD71^{hi}$ and $CD105^{hi}$ cells were significantly reduced in −Epo cultures (Figure 1C and F). This decrease was accompanied by an increase in

CD71$^{lo}$ but not CD105$^{lo}$ cells. This scaled expression and Epo-dependence was observed with CD71 and CD105 antibodies labeled with two different fluorophores and has been reported in previous studies (Figure 1 and S4) [21,22,24-26,29,44]. Overall, the results confirmed the Epo-dependent development of erythroblasts in our culture system and indicated Epo's influence on the surface expression of CD71 and CD105.

**Immunophenotypic Resolution of Early Erythroid Progenitors**

Utilizing previously described markers, we developed an immunophenotyping strategy for monitoring the Epo-dependent transition within EE progenitors, BFU-E and CFU-E (Figure 2). First, CD3, CD10, CD19, CD11b, CD41, and CD123 were used to gate out non-erythroid lineages and progenitors; CMP and GMP are both expected to be CD123 positive and therefore, should be eliminated with this panel. From the LiveLin$^{-}$CD123$^{-}$ cells, CD71$^{+}$CD235a$^{-}$ cells were then selected and from this population, only CD49d$^{+}$CD117$^{+}$ cells were considered for further analysis, since these markers have been shown to be expressed in EE progenitors (Figure 2A i and ii) [22,25]. As BFU-E, but not CFU-E, are expected to express CD34, all CD105$^{+}$ cells were segregated based on CD34 positivity (Figure 2A iii). Therefore, all EE cells were LiveLin$^{-}$CD123$^{-}$CD235a$^{-}$CD71$^{+}$CD49d$^{+}$CD117$^{+}$, and within this population, total BFU-E were additionally CD34$^{+}$CD105$^{+}$, whereas total CFU-E were CD34$^{-}$CD105$^{+}$. Further stratification of total BFU-E and CFU-E populations based on CD105 and CD71 expression resolved heterogeneity within them (Figure 2A iv and v). BFU-E consisted of two populations: a large CD34$^{+}$CD71$^{lo}$CD105$^{lo}$ population and another smaller CD34$^{+}$CD71$^{hi}$CD105$^{lo}$ population that were termed early BFU-E (earlyB) and late BFU-E (lateB), respectively. Within CFU-E, three populations emerged: CD34$^{-}$CD71$^{lo}$CD105$^{lo}$ early CFU-E (earlyC), CD34$^{-}$CD71$^{hi}$CD105$^{lo}$ mid CFU-E (midC), and CD34$^{-}$CD71$^{hi}$CD105$^{hi}$ late CFU-E (lateC) (Table S1).

Assessment of CD36, which has previously been employed to distinguish BFU-E and CFU-E cells, showed that amongst BFU-E, the fraction of CD36$^{+}$ cells was markedly higher in lateB (~59%) than in earlyB (~1.5%) (Figure 3A i and ii, and 3C) [23,45,46]. Within CFU-E, the CD36$^{+}$ cells increased from ~25% in earlyC to ~81% in midC and ~99% in lateC (Figure 3A iii-v, and 3C). These results indicate that within the EE compartment, there is a continuum of cells that are simultaneously losing CD34 and gaining CD36 expression. The observed patterns of CD34, CD71, CD105, and CD36 suggest the existence of two alternative differentiation routes (Figure 3D). In one route, loss of CD34 and gradual gain of CD36 transition earlyB to earlyC, both of which are CD71$^{lo}$CD105$^{lo}$. EarlyC then sequentially differentiate through midC and lateC. In the other route, the onset of CD36 expression precedes the downregulation of CD34, leading to the transition of earlyB to lateB, that are CD71$^{hi}$CD105$^{lo}$. In this alternative route, the earlyC stage is likely bypassed, with lateB transitioning directly to midC, which form lateC.

To confirm that the observed stratification of EE cells was not an artifact of the combination of fluorophores that were used in the antibody panel, we designed a second panel in which CD49d, CD71, CD105, and CD36 antibodies were conjugated to different fluorophores (Figure S4A, C, and E). The list of antibodies for the two panels are provided in Table S2. Application of the second panel also demonstrated the presence of five EE populations at percentages similar to those observed with the initial fluorophore combination (Figure S4C and S5). Additionally, the pattern of CD36 expression was also similar to that seen with the first panel (Figure S4E). Put together, these results confirm that heterogeneity within EE cells can be resolved based on CD71 and CD105 expression and that the rates of CD34 downregulation and CD36 upregulation may vary within each cell.

**Erythropoietin is Required for the Development of Late CFU-E**

To examine the role of Epo in population dynamics within EE, cells from BM-derived $CD34^+$ HSPCs cultured in +Epo medium were compared to those cultured in −Epo medium by immunophenotyping. Assessment of total BFU-E in +Epo culture showed an increase from day 4 to 7, which was followed by maintenance of their levels until day 10; this trend was largely sustained in the absence of Epo (Figures 2A iii, B iii, and C). In line with this observation, percentages of earlyB and lateB were also unaffected by the absence of Epo (Figures 2A iv, B iv, D, and E). The levels of total CFU-E, on the other hand, decreased steadily from day 4 to 10 in +Epo conditions (Figure 2F). Although CD235a expression indicated an increase in total erythroblasts (Figure S1), there was some variability in the trend exhibited by the individual erythroblast populations (Figures 2G-H). The percentage of OrthoE, the final erythroblast stage, increased steadily, indicating a continuous transition through TED (Figure 2H). In the absence of Epo, however, there was a significant decrease in total CFU-E on days 4 and 7 of culture (Figures 2A iii, B iii, and F). The lack of difference in CFU-E percentages in +Epo and −Epo conditions on day 10 is likely due to their progression into TED in the presence of Epo. Interestingly, examination of the individual CFU-E populations revealed differential effects within the subtypes. The percentage of lateC was significantly lower in −Epo compared to +Epo cultures on all three days of assessment, whereas the percentages of both earlyC and midC were higher in the absence of Epo (Figures 2A v, B v, and I-K). These differences in early and midC were significant only on day 4 and not at later timepoints, most likely due to the continued differentiation of CFU-E in +Epo cultures. These results suggest that a lack of Epo reduces the production of lateC with concomitant accumulation of earlyC and midC. The absence of Epo did not have a significant effect on earlyB and lateB or their transition to earlyC or midC, respectively. Similarly, analysis using the second antibody panel indicated comparable percentages of EE cells, absence of an effect of Epo on total BFU-E and BFU-E subpopulations, and an accumulation of earlyC accompanied by reduced production of lateC in cultures lacking Epo (Figures S4C-D and S5).

In previous studies, BFU-E and CFU-E have been characterized as $CD34^+CD36^-$ and $CD34^-CD36^+$, respectively [23,44]. Interestingly, examination by both antibody panels employed in this study showed that CD36 expression within BFU-E and CFU-E populations was unaffected by the absence of Epo (Figures 3A-B, S3, and S4E-F). Further, application of the strategy proposed by Li et al. for the analysis of EE populations in +Epo and −Epo cultures failed to resolve Epo-dependence (Figure S6A). Furthermore, Yan et al. demonstrated heterogeneity within EE progenitors and proposed strategies for resolution of progenitors and erythroblasts [21,22]. Based on the assessment of CD105 and CD235a, we were able to recapitulate the erythroblast populations within the $CD235a^+$ cells (Figure S1C). However, we were unable to separate the BFU-E and CFU-E populations based on the patterns of CD34 and CD105 (Figure S6B). This could be because a $CD34^+$ population that was $CD105^{hi}$ was not observed in our culture system.

**All BFU-E and CFU-E Subtypes are Present in Human Bone Marrow**

To ascertain that all observed EE subtypes were present in human BM, we performed prospective analyses. For BFU-E, frozen BM $CD34^+$ cells were incubated overnight in stimulation medium, which does not contain Epo, and then analyzed by immunophenotyping (Table S1). Examination of CD34 expression revealed that >90% of the cells were $CD34^+$, suggesting that the short overnight incubation did not result in significant progression beyond the HSPC stages. Immunophenotyping of these cells exhibited the presence of earlyB and lateB, with the percentage of lateB being slightly higher than that seen in BM $CD34^+$ cell cultures (Figure 4A). To analyze CFU-E subtypes, total BM mononuclear cells (MNCs) were also immunophenotyped after an overnight incubation in stimulation medium. This analysis

revealed the presence of both BFU-E and all three CFU-E populations in BM MNCs (Figure 4B). Thus, all EE populations were prospectively discernible in BM cells.

**Isolated Early Erythroid Populations Exhibit Expected Differentiation Trajectories**

To further investigate the differentiation potential of each of the five EE populations, they were sorted on day 4 by fluorescence activated cell sorting (FACS) and recultured in suspension for immunophenotypic analysis and in semi-solid media for colony forming cell (CFC) assays. In initial attempts, the numbers of earlyC and midC were found to be insufficient for downstream analysis, so they were sorted together. For suspension cultures, sorted cells were replated in complete medium containing Epo. During reculture, proliferation was observed to be highest for earlyB and lowest for lateC, while lateB and earlyC/midC exhibited similar intermediate expansion capacity (Figure S7A). On day 4, immunophenotyping of cells from cultures of sorted earlyB detected mostly earlyB, but by day 7, a large number of earlyC were seen, along with a few midC, lateC, and erythroblasts as well (Figure 5A). Sorted lateB, on the other hand, produced primarily lateB, midC, and lateC on day 4, which progressed to all erythroblast populations by day 7 (Figure 5B). Notably, earlyC were not observed in cultures of sorted lateB, thereby indicating that lateB may be transitioning directly to midC. Reculture of the earlyC/midC pool yielded all CFU-E populations and all erythroblast populations, with mainly ProE and BasoE arising by day 4 and PolyE and OrthoE forming by day 7 (Figure 5C). Sorted lateC also efficiently produced erythroblasts (Figure 5D). MidC and lateC were still present in lateB cultures on day 7, while this was not the case for cultures of earlyC/midC or lateC, because all cells had entered TED, as seen in the erythroblast scatter plots (Figures 5B-D). These results demonstrate the proliferation and erythroid differentiation potential of the sorted individual EE populations. Further, the inability of sorted lateB to produce earlyC supports the presence of two differentiation routes (Figure 3D).

For additional functional analysis by CFC assays, the isolated EE cells were plated in semisolid medium containing either all cytokines (including Epo) or Epo alone, as conventionally, CFU-E have been characterized by their ability to form colonies in Epo-only medium [22,23,47]. Analysis of colonies formed by unsorted cells harvested on day 4 of culture confirmed the ability of semisolid medium to support the formation of colony-forming unit granulocyte-monocyte (CFU-GM), BFU-E, and CFU-E colonies (Figures 6A-B and S7B). As previously reported, two types of BFU-E colonies were observed: large colonies that consisted of multiple clusters of hemoglobinized cells (large BFU-E) and smaller single cluster colonies that were visible at 40x (small BFU-E) [47,48]. The CFU-E colonies, on the other hand, were difficult to visualize at 40x, but easily seen at 100x (Figures 6A-B).

Examination of colonies formed from the sorted EE populations showed that earlyB formed small and large BFU-E colonies in complete medium and did not produce any colonies on Epo-only plates (Figure 6C). Interestingly, earlyB also formed CFU-GM colonies, indicating some plasticity. LateB formed both small and large BFU-E and CFU-E colonies in complete medium; surprisingly, they also produced CFU-E colonies in Epo-only medium (Figure 6D). While the earlyC/midC mix produced small BFU-E and CFU-E colonies in complete medium, they also formed CFU-E colonies in Epo-only medium (Figure 6E). The last EE population, lateC, yielded primarily CFU-E colonies in both types of media (Figure 6F). These results suggest that earlyB, which are $CD34^{+}CD71^{lo}CD105^{lo}$ but largely $CD36^{-}$ exhibit some plasticity, retaining the ability to form CFU-GM colonies. Other studies have also reported the formation of GM colonies from sorted BFU-E [22,23,49]. The other four EE populations are strictly erythroid lineage committed. They also suggest that lateB and earlyC/midC populations, representing transitional stages, form similar types of colonies. The lateC represent a subset of $CD34^{-}CD36^{+}$

cells that only form CFU-E colonies and have completed the EE transition but have not yet entered TED, as they are CD235a$^{-}$.

In the CFC-assays, we noted the formation of CFU-E colonies by sorted lateB and earlyC/midC mix, in complete medium and surprisingly, also in Epo only medium. Like lateC, these two subpopulations are CD36$^{+}$. To examine if CD36 expression was a determinant in colony phenotype, total BFU-E (Lin$^{-}$CD123$^{-}$CD235a$^{-}$CD71$^{+}$CD49d$^{+}$CD117$^{+}$CD34$^{+}$CD105$^{+}$) and CFU-E (Lin$^{-}$CD123$^{-}$CD235a$^{-}$CD71$^{+}$CD49d$^{+}$CD117$^{+}$CD34$^{-}$CD105$^{+}$) were sorted based on CD36 into four populations—CD36$^{+}$-BFU-E, CD36$^{-}$-BFU-E, CD36$^{+}$-CFU-E, and CD36$^{-}$-CFU-E—and plated in either complete or Epo alone medium. In this analysis, CD36$^{-}$-BFU-E exhibited the ability to form CFU-GM colonies and formed large and small BFU-E colonies in complete medium but did not form any colonies in Epo only medium (Figure 6G-H). CD36$^{+}$-BFU-E did not form CFU-GM but formed large and small BFU-E and CFU-E colonies. Interestingly, CD36$^{+}$-BFU-E formed CFU-E colonies also in Epo-only medium (Figure 6H). CD36$^{-}$-CFU-E primarily formed large and small BFU-E colonies in complete medium and none in Epo-only medium. CD36$^{+}$-CFU-E formed small BFU-E and CFU-E colonies in complete medium, and just CFU-E colonies in Epo-only medium. The ability of sorted CD36$^{+}$-BFU-E and CD36$^{+}$-CFU-E, but not CD36$^{-}$-BFU-E and CD36$^{-}$-CFU-E, to form CFU-E colonies suggests that CD36 expression may be associated with the CFU-E colony phenotype. Additionally, the ability of CD36$^{-}$-BFU-E but not of CD36$^{+}$-BFU-E to form CFU-GM colonies suggests that CD36 expression may be linked to loss of plasticity. Overall, analysis by reculturing and CFC assays confirmed the potential of the isolated EE progenitor subtypes to progress along the erythroid trajectory and supported the existence of two parallel routes, one of which transitions through earlyC and the other through lateB, and also indicated a role for CD36 in determining the CFU-E colony phenotype.

**Occurrence of EE Subtypes During Neonatal Erythroid Differentiation**

To examine if the EE subpopulations were detectable during neonatal erythroid differentiation, we cultured CB-derived CD34$^{+}$ HSPCs in +Epo and −Epo conditions. Immunophenotyping of the CB cultures revealed similar EE population dynamics as observed for BM cultures (Figure 2). As such, the expression CD235a and all erythroblast populations were seen only in +Epo cultures (Figure S8). There was also a significant decrease in the percentage of CD71$^{hi}$, CD105$^{hi}$, and CD36$^{+}$ cells and an accumulation of CD71$^{lo}$ cells in the absence of Epo (Figure S9 and S10E-F). Furthermore, all five EE populations identified in BM cells were also resolved in CB cultures (Figure 7A). As with BM, the absence of Epo did not affect the formation of BFU-E, total or the subtypes (Figure 7A-B and S11). There was also a drastic and significant decrease in lateC formation in the absence of Epo that was accompanied by the accumulation of earlyC but not midC, thereby suggesting the Epo-dependence of lateC formation also in the neonatal system (Figure 7A-E). Finally, as with BM-derived cells, CD36$^{+}$ cells were <2% within earlyB but rose to ~50% in lateB and also rose within CFU-E subtypes from ~20% in earlyC, ~90% in midC, and essentially 100% in lateC (Figure S12). CD36 expression within each population was still not affected by the absence of Epo.

To discern any differences in erythroid population dynamics between adult and neonatal populations, we simultaneously cultured BM- and CB-derived cells in complete medium containing Epo. Assessment of marker expression and cell stage progression on days 4, 7, and 10 revealed similar percentages of individual markers, the BFU-E and CFU-E subpopulations, and CD36 expression within them (Figure S13). Comparison of erythroblast populations revealed a significantly higher percentage of ProE and early BasoE in the adult BM cultures than in neonatal CB cultures, although the differences in percentages were relatively low (Figure S14A-B). These results likely indicate a slightly delayed entry into TED in CB cultures, which is in alignment with a previously reported study comparing in PB (adult) and CB cultures [21]. Overall, the analysis demonstrates that, as with differentiation of BM CD34$^{+}$ cells, the five EE

subpopulations arise during the differentiation of CB $CD34^+$ cells and likely progress through two differentiation paths.

## Discussion

By immunophenotyping of transiently expressed markers on cells from *ex vivo* cultures of BM-derived HSPCs, we resolved heterogeneous EE progenitor populations and identified the key Epo-dependent transition (Figure 7F). Based on the expression patterns of CD34, CD71, and CD105 within $Lin^-CD123^-CD235a^-CD71^+CD49d^+CD117^+$ cells, we detect five EE subtypes: two BFU-E and three CFU-E. The two BFU-E, earlyB and lateB are $CD34^+$ but can be distinguished as $CD71^{lo}CD105^{lo}$ and $CD71^{hi}CD105^{lo}$, respectively. The CFU-E earlyC, midC, and lateC, are $CD34^-$ and distinguishable as $CD71^{lo}CD105^{lo}$, $CD71^{hi}CD105^{lo}$, and $CD71^{hi}CD105^{hi}$, respectively. Additionally, prospective analysis detected the two BFU-E subtypes and three CFU-E subtypes in BM cells, and after isolation, each individual population exhibited the capacity to continue differentiation along the erythroid route. Furthermore, all five EE populations were also resolved in *ex vivo* cultures of CB-derived HSPCs at levels similar to those observed in BM cultures. Importantly, Epo was found to be essential for the acquisition of the $CD71^{hi}CD105^{hi}$ immunophenotype during the midC to lateC transition in both BM and CB. Expression pattern of CD71, CD105, and CD36 allowed us to decipher two routes to lateC formation (Figure 7F). In the first, loss of CD34 expression occurs prior to the gain of CD36 and progresses from earlyB→earlyC→midC→lateC. The second pathway, on the other hand, bypasses earlyC because of onset of CD36 expression in $CD34^+$ cells, and the progression follows from earlyB→lateB→midC→lateC.

Although not entirely Epo-dependent, both CD71 and CD105 are dynamically expressed and sensitive to Epo in EE cells. While the function of CD71 (transferrin receptor) is well characterized, the role played by CD105 (endoglin) in erythroid differentiation is less clear [50,51]. Also known as transforming growth factor β (TGF-β) receptor type III, CD105 associates with type I and II receptors upon binding of TGF-β superfamily ligands to regulate gene expression via Smad signaling [52-54]. In mice, CD105 loss was reported to be associated with decreased erythroid output and a potential role in regulating proliferation of BFU-E and BasoE [55,56]. Expression of CD105 on immature human erythroid cells has been known for a long time, and its increase in MEP has been positively corelated with erythroid commitment [26,57]. We observed a basal level of CD105 on MEP, CMP, and GMP by flow cytometry (Schippel and Sharma, unpublished data). Notably, a $CD71^{hi}CD105^{hi}$ mature CFU-E population within the $CD34^+CD36^+$ compartment was reported in human PB-, CB-, and BM-derived cells [31]. LateC identified in the present study is $CD34^-$, thus different from the mature $CD34^+CD36^+$ CFU-E. Further characterization of target genes and cellular processes regulated by CD105 is needed to understand its precise role in EE cells.

In several studies, CD36 has been proposed to mark commitment to the erythroid lineage [24-27,29,58]. The onset of CD36 expression has been shown to be accompanied by the loss of CD34 during the BFU-E to CFU-E transition [23,30]. During differentiation of human PB $CD34^+$ cells, a $CD34^+CD36^+$ population that gives rise to BFU-E and CFU-E was identified [21]. Accumulation of a $CD34^+CD36^+$ population has also been detected in the PB of patients with hypercortisolemia and is associated with unresponsiveness to dexamethasone, a synthetic glucocorticoid commonly used for anemia treatment [30-32]. In our study, the $CD34^+CD36^+$ lateB were identified as an intermediate population that forms in an Epo-independent manner and transitions directly to the $CD34^-CD36^+$ midC. Interestingly, humans lacking CD36 protein due to genetic mutations generally develop normally, but have thrombocytopenia, increased

bleeding, and RBC abnormalities such as higher RBC distribution width (RDW) [59-61]. CD36 knockout mice develop normally, although they also have thrombocytopenia, along with slight but significantly reduced RBC counts [62]. In contrast, in *ex vivo* experiments, $CD34^+$ HSPCs from an individual lacking CD36 were found to undergo erythroid commitment and differentiation without much effect on either CD71 and CD235a expression or erythroblast development, as assessed by CD49d ($\alpha$-4 Integrin) and CD233 (Band 3) expression according to the strategy proposed by Hu et al. [24,63]. However, whether CD36 loss affects other markers such as CD105 or the enucleation and maturation of erythroblasts remains to be determined. Our CFC analysis showed a potential link between CD36 expression and the CFU-E phenotype. Ability of lateB and earlyC/midC to form CFU-E colonies in Epo only medium suggests that expression of CD36 may represent a step beyond which erythroid cells lose plasticity and require only Epo as an extracellular cytokine signal to progress through TED. Thus, CD36 may be sufficient to confer independence from other cytokines but not Epo. Additional analysis is needed to functionally characterize the role of CD36 during EE.

Anemia is a common health condition that can arise due to a multitude of health conditions, including iron or vitamin deficiency, inherited RBC disorders, infections (such as malaria), obstetric-gynecological conditions, and chronic diseases that lead to dysregulated erythropoiesis [64,65]. Administration of recombinant human Epo and dexamethasone are prevalent treatments for anemia; however, they are not always effective, and the observed improvements are often temporary [66,67]. Thus, there is a significant need to advance the knowledge of Epo's influence on EE populations. Our study provides a framework for investigations into regulation of key developmental stages by other factors that may promote erythroid differentiation to aid the identification of new therapeutic targets.

## Materials and Methods

### Culture and Differentiation of $CD34^+$ HSPCs

Human BM-derived $CD34^+$ HSPCs and MNCs, all from female donors between the age 13 to 34 years, were purchased from Ossium Health (San Francisco, CA, USA) and Stem Cell Technologies (Vancouver, BC, Canada), respectively. For all donor samples, quality control by flow cytometry indicating >90% viability, via staining with 7AAD, and >90% CD34 positivity, using CD45 and CD34 antibody staining, was provided by supplier and confirmed by in-house immunophenotyping analysis. Furthermore, tests indicating negative results for HIV1/2 antibody, HBV surface antigen, HBV core antibody, HCV antibody, HIV/HBV/HCV nucleic acid amplification, cytomegalovirus, and syphilis were provided for all donor cells. CB units were obtained from Valleywise Health hospital, Arizona through a material transfer agreement. $CD34^+$ HSPCs were isolated as previously described [40-42]. MS-5 cells (used as feeder cells for co-culture with $CD34^+$ HSPCs) were maintained in Dulbecco's modified Eagle's medium (DMEM) with high glucose and L-glutamine (Thermo Fisher Scientific, Waltham, MA), 10% fetal bovine serum (FBS; negative for mycoplasma; Omega Scientific, Tarzana, CA), and 1% penicillin-streptomycin (Pen-Strep, Sigma-Aldrich, St. Louis, MO). MS-5 cells are checked annually for absence of mycoplasma contamination.

Culture of BM and CB $CD34^+$ HSPCs was performed as previously described [40-42]. Briefly, HSPCs were incubated overnight at a density of $1 \times 10^5$ cells/well of a 48-well plate in 200 $\mu$L of stimulation medium (serum-free X-VIVO 15 (Lonza, Basel, Switzerland) containing 2

mM L-glutamine, 50 ng/mL stem cell factor (SCF), 50 ng/mL thrombopoietin (TPO), 20 ng/mL interleukin-3 (IL-3), and 50 ng/mL Flt3-Ligand (Flt-3)). The stimulated $CD34^+$ cells were collected and plated onto MS-5 cells at a density of 3 x $10^4$ cells/well of a 48-well plate for analysis on day 4 and 1 x $10^4$ cells/well for analysis on day 7 or 10 in complete medium (DMEM with high glucose and L-glutamine, 10% FBS, and 1% Pen-Strep, supplemented with 50ng/mL Tpo (Miltenyi Biotec, Auburn, CA), 5ng/mL SCF, 5ng/mL IL-3, and 5ng/mL Flt-3, with or without 4U/mL Epo (BioBasic, Amherst, NY or StemCell Technologies). Half-medium change was performed on days 4 and 7.

For reculture experiments, the individual EE cells were sorted into complete medium (containing Epo) supplemented with 20% FBS as described below. The sorted cells were counted and plated on MS-5 cells at a density of either 3 x $10^4$ cells/200 μL or 1 x $10^4$ cells/200 μL/well in a 48-well plate in complete medium and incubated as described above.

**Immunophenotyping and Cell Sorting**

For flow cytometry analyses, cells were harvested and stained with fluorescently labeled antibodies as previously described [40-42]. Briefly, cells were washed and resuspended in phosphate-buffered saline (PBS), counted using the Countess 3-FL Automated Cell Counter (Thermo Fisher Scientific, Waltham, MA), and then stained with an antibody cocktail, as indicated in the figures. Stained cells were washed with PBS, fixed with 1% paraformaldehyde (PFA) (Sigma Aldrich, St. Louis, Missouri), and resuspended in flow cytometry (FC) buffer (PBS containing 2% FBS and 5 mM EDTA). Single stained controls were prepared using compensation beads (UltraComp eBeads from Thermo Fisher Scientific, Waltham, MA) as per the manufacturer's recommendations. All flow cytometry analysis was performed on a Canto II (BD Biosciences, San Jose, CA), and data was analyzed using FlowJo (version 10.9.0).

For FACS, cells were collected on day 4 of culture, washed, counted, and stained as described above. Stained cells were washed and resuspended in FC buffer at a density of 3-5 x $10^6$ cells/mL and then sorted into four populations (earlyB, lateB, earlyC/midC, and lateC) based on immunophenotypes (Table S1) using a FACS Aria II (BD Biosciences, San Jose, CA) into complete medium supplemented with 20% FBS. Sorted cells were counted and plated either in complete myeloid medium for re-culture or in semisolid medium for CFC assays.

**Colony Forming Cell Assay**

For CFC assays, MethoCult® classic (H4434), classic without Epo (H4534), Epo-only (H4330), or without cytokines (H4230) were used (STEMCELL Technologies; Cambridge, MA). Cells were diluted to a density of 2.5–5 x $10^3$ cells/mL in MethoCult medium and plated in triplicate in 35 mm tissue culture dishes. After 14 days of incubation, colonies were counted and characterized based on criteria described by Palis and Koniski [47]. Images were obtained using an Olympus IX2-SP inverted microscope under 40x and 100x magnification.

**Statistical Analysis**

At least three biological replicates were performed for each experiment; each biological replicate represented a unique HSPC donor. The exact number of replicates for individual experiments is indicated in figure legends. Graphical representation plots and statistical analysis by student T-test were performed in GraphPad Prism (version 10.0.3; La Jolla, CA). Data is represented as mean ± standard error of the mean (SEM) and p values $<0.05$ were considered significant.

**Acknowledgments**

The authors would like to acknowledge funding support to SS from the National Institutes of General Medical Sciences (R01GM127464) and National Cancer Institute (P30CA023074) of the National Institutes of Health, the Valley Research Partnership Program (VRP P1-4009 and VRP77), and the Arizona Biomedical Research Center (ABRC: RFGA2022-010-30). The content is solely the responsibility of the authors and does not necessarily represent the official views of the National Institute of Health.

## References


1 Bunn HF. Erythropoietin. Cold Spring Harb Perspect Med 2013;3(3):a011619.
2 Bhoopalan SV, Huang LJ, Weiss MJ. Erythropoietin regulation of red blood cell production: from bench to bedside and back. F1000Res 2020;9.
3 Valent P, Busche G, Theurl I et al. Normal and pathological erythropoiesis in adults: from gene regulation to targeted treatment concepts. Haematologica 2018;103(10):1593-1603.
4 Grover A, Mancini E, Moore S et al. Erythropoietin guides multipotent hematopoietic progenitor cells toward an erythroid fate. J Exp Med 2014;211(2):181-188.
5 Iscove NN, Guilbert LJ. Erythropoietin-Independence of Early Erythropoiesis and a Two-Regulator Model of Proliferative Control in the Hemopoietic System. In: Murphy MJ, Peschle C, Gordon AS et al., eds. In Vitro Aspects of Erythropoiesis. New York, NY: Springer US, 1978:3-7.
6 Lin CS, Lim SK, D'Agati V et al. Differential effects of an erythropoietin receptor gene disruption on primitive and definitive erythropoiesis. Genes Dev 1996;10(2):154-164.
7 Malik J, Kim AR, Tyre KA et al. Erythropoietin critically regulates the terminal maturation of murine and human primitive erythroblasts. Haematologica 2013;98(11):1778-1787.
8 Kieran MW, Perkins AC, Orkin SH et al. Thrombopoietin rescues in vitro erythroid colony formation from mouse embryos lacking the erythropoietin receptor. Proc Natl Acad Sci U S A 1996;93(17):9126-9131.
9 Wu H, Liu X, Jaenisch R et al. Generation of committed erythroid BFU-E and CFU-E progenitors does not require erythropoietin or the erythropoietin receptor. Cell 1995;83(1):59-67.
10 Mulcahy L. The erythropoietin receptor. Semin Oncol 2001;28(2 Suppl 8):19-23.
11 Witthuhn BA, Quelle FW, Silvennoinen O et al. JAK2 associates with the erythropoietin receptor and is tyrosine phosphorylated and activated following stimulation with erythropoietin. Cell 1993;74(2):227-236.
12 Tsiftsoglou AS. Erythropoietin (EPO) as a Key Regulator of Erythropoiesis, Bone Remodeling and Endothelial Transdifferentiation of Multipotent Mesenchymal Stem Cells (MSCs): Implications in Regenerative Medicine. Cells 2021;10(8).
13 Tothova Z, Semelakova M, Solarova Z et al. The Role of PI3K/AKT and MAPK Signaling Pathways in Erythropoietin Signalization. Int J Mol Sci 2021;22(14).
14 Tothova Z, Tomc J, Debeljak N et al. STAT5 as a Key Protein of Erythropoietin Signalization. Int J Mol Sci 2021;22(13).
15 Kuhrt D, Wojchowski DM. Emerging EPO and EPO receptor regulators and signal transducers. Blood 2015;125(23):3536-3541.
16 Schippel N, Sharma S. Dynamics of human hematopoietic stem and progenitor cell differentiation to the erythroid lineage. Exp Hematol 2023;123:1-17.
17 Tur S, Palii CG, Brand M. Cell fate decision in erythropoiesis: Insights from multiomics studies. Exp Hematol 2024;131:104167.
18 Hattangadi SM, Wong P, Zhang L et al. From stem cell to red cell: regulation of erythropoiesis at multiple levels by multiple proteins, RNAs, and chromatin modifications. Blood 2011;118(24):6258-6268.
19 Dzierzak E, Philipsen S. Erythropoiesis: development and differentiation. Cold Spring Harb Perspect Med 2013;3(4):a011601.
20 An X, Schulz VP, Mohandas N et al. Human and murine erythropoiesis. Curr Opin Hematol 2015;22(3):206-211.
21 Yan H, Hale J, Jaffray J et al. Developmental differences between neonatal and adult human erythropoiesis. Am J Hematol 2018;93(4):494-503.

22 Yan H, Ali A, Blanc L et al. Comprehensive phenotyping of erythropoiesis in human bone marrow: Evaluation of normal and ineffective erythropoiesis. Am J Hematol 2021;96(9):1064-1076.
23 Li J, Hale J, Bhagia P et al. Isolation and transcriptome analyses of human erythroid progenitors: BFU-E and CFU-E. Blood 2014;124(24):3636-3645.
24 Hu J, Liu J, Xue F et al. Isolation and functional characterization of human erythroblasts at distinct stages: implications for understanding of normal and disordered erythropoiesis in vivo. Blood 2013;121(16):3246-3253.
25 Wangen JR, Eidenschink Brodersen L, Stolk TT et al. Assessment of normal erythropoiesis by flow cytometry: important considerations for specimen preparation. Int J Lab Hematol 2014;36(2):184-196.
26 Mori Y, Chen JY, Pluvinage JV et al. Prospective isolation of human erythroid lineage-committed progenitors. Proc Natl Acad Sci U S A 2015;112(31):9638-9643.
27 Machherndl-Spandl S, Suessner S, Danzer M et al. Molecular pathways of early CD105-positive erythroid cells as compared with CD34-positive common precursor cells by flow cytometric cell-sorting and gene expression profiling. Blood Cancer J 2013;3:e100.
28 Loken MR, Shah VO, Dattilio KL et al. Flow cytometric analysis of human bone marrow: I. Normal erythroid development. Blood 1987;69(1):255-263.
29 Fajtova M, Kovarikova A, Svec P et al. Immunophenotypic profile of nucleated erythroid progenitors during maturation in regenerating bone marrow. Leuk Lymphoma 2013;54(11):2523-2530.
30 Iskander D, Psaila B, Gerrard G et al. Elucidation of the EP defect in Diamond-Blackfan anemia by characterization and prospective isolation of human EPs. Blood 2015;125(16):2553-2557.
31 Ashley RJ, Yan H, Wang N et al. Steroid resistance in Diamond Blackfan anemia associates with p57Kip2 dysregulation in erythroid progenitors. J Clin Invest 2020;130(4):2097-2110.
32 Varricchio L, Geer EB, Martelli F et al. Patients with hypercortisolemic Cushing disease possess a distinct class of hematopoietic progenitor cells leading to erythrocytosis. Haematologica 2023;108(4):1053-1067.
33 Bhoopalan SV, Yen JS, Mayuranathan T et al. An RPS19-edited model for Diamond-Blackfan anemia reveals TP53-dependent impairment of hematopoietic stem cell activity. JCI Insight 2023;8(1).
34 Bauer K, Machherndl-Spandl S, Kazianka L et al. CAR virus receptor mediates erythroid differentiation and migration and is downregulated in MDS. Leukemia 2023;37(11):2250-2260.
35 Papoin J, Yan H, Leduc M et al. Phenotypic and proteomic characterization of the human erythroid progenitor continuum reveal dynamic changes in cell cycle and in metabolic pathways. Am J Hematol 2024;99(1):99-112.
36 Palii CG, Cheng Q, Gillespie MA et al. Single-Cell Proteomics Reveal that Quantitative Changes in Co-expressed Lineage-Specific Transcription Factors Determine Cell Fate. Cell Stem Cell 2019;24(5):812-820 e815.
37 Pronk CJ, Rossi DJ, Mansson R et al. Elucidation of the phenotypic, functional, and molecular topography of a myeloerythroid progenitor cell hierarchy. Cell Stem Cell 2007;1(4):428-442.
38 Swaminathan A, Hwang Y, Winward A et al. Identification and Isolation of Burst-Forming Unit and Colony-Forming Unit Erythroid Progenitors from Mouse Tissue by Flow Cytometry. J Vis Exp 2022(189).
39 Tusi BK, Wolock SL, Weinreb C et al. Population snapshots predict early haematopoietic and erythroid hierarchies. Nature 2018;555(7694):54-60.

40 Bapat A, Schippel N, Shi X et al. Hypoxia promotes erythroid differentiation through the development of progenitors and proerythroblasts. Exp Hematol 2021;97:32-46 e35.
41 Bapat A, Keita N, Sharma S. Pan-myeloid Differentiation of Human Cord Blood Derived CD34+ Hematopoietic Stem and Progenitor Cells. J Vis Exp 2019(150).
42 Bapat A, Keita N, Martelly W et al. Myeloid Disease Mutations of Splicing Factor SRSF2 Cause G2-M Arrest and Skewed Differentiation of Human Hematopoietic Stem and Progenitor Cells. Stem Cells 2018;36(11):1663-1675.
43 Violidaki D, Axler O, Jafari K et al. Analysis of erythroid maturation in the nonlysed bone marrow with help of radar plots facilitates detection of flow cytometric aberrations in myelodysplastic syndromes. Cytometry B Clin Cytom 2020;98(5):399-411.
44 Gautier EF, Ducamp S, Leduc M et al. Comprehensive Proteomic Analysis of Human Erythropoiesis. Cell Rep 2016;16(5):1470-1484.
45 Nakahata T, Okumura N. Cell surface antigen expression in human erythroid progenitors: erythroid and megakaryocytic markers. Leuk Lymphoma 1994;13(5-6):401-409.
46 Okumura N, Tsuji K, Nakahata T. Changes in cell surface antigen expressions during proliferation and differentiation of human erythroid progenitors. Blood 1992;80(3):642-650.
47 Palis J, Koniski A. Functional Analysis of Erythroid Progenitors by Colony-Forming Assays. Methods Mol Biol 2018;1698:117-132.
48 Gregory CJ, Eaves AC. Human marrow cells capable of erythropoietic differentiation in vitro: definition of three erythroid colony responses. Blood 1977;49(6):855-864.
49 Abovich N, Liao XC, Rosbash M. The yeast MUD2 protein: an interaction with PRP11 defines a bridge between commitment complexes and U2 snRNP addition. Genes Dev 1994;8(7):843-854.
50 Moura IC, Hermine O, Lacombe C et al. Erythropoiesis and transferrin receptors. Curr Opin Hematol 2015;22(3):193-198.
51 Richard C, Verdier F. Transferrin Receptors in Erythropoiesis. Int J Mol Sci 2020;21(24).
52 Zhang L, Magli A, Catanese J et al. Modulation of TGF-beta signaling by endoglin in murine hemangioblast development and primitive hematopoiesis. Blood 2011;118(1):88-97.
53 Meurer SK, Weiskirchen R. Endoglin: An 'Accessory' Receptor Regulating Blood Cell Development and Inflammation. Int J Mol Sci 2020;21(23).
54 Schoonderwoerd MJA, Goumans MTH, Hawinkels L. Endoglin: Beyond the Endothelium. Biomolecules 2020;10(2).
55 Moody JL, Singbrant S, Karlsson G et al. Endoglin is not critical for hematopoietic stem cell engraftment and reconstitution but regulates adult erythroid development. Stem Cells 2007;25(11):2809-2819.
56 Cho SK, Bourdeau A, Letarte M et al. Expression and function of CD105 during the onset of hematopoiesis from Flk1(+) precursors. Blood 2001;98(13):3635-3642.
57 Buhring HJ, Muller CA, Letarte M et al. Endoglin is expressed on a subpopulation of immature erythroid cells of normal human bone marrow. Leukemia 1991;5(10):841-847.
58 Orfao A, Matarraz S, Perez-Andres M et al. Immunophenotypic dissection of normal hematopoiesis. J Immunol Methods 2019;475:112684.
59 Barrachina MN, Pernes G, Becker IC et al. Efficient megakaryopoiesis and platelet production require phospholipid remodeling and PUFA uptake through CD36. bioRxiv 2023.
60 Chami N, Chen MH, Slater AJ et al. Exome Genotyping Identifies Pleiotropic Variants Associated with Red Blood Cell Traits. Am J Hum Genet 2016;99(1):8-21.

61 Auer PL, Johnsen JM, Johnson AD et al. Imputation of exome sequence variants into population- based samples and blood-cell-trait-associated loci in African Americans: NHLBI GO Exome Sequencing Project. Am J Hum Genet 2012;91(5):794-808.
62 Barrachina MN, Pernes G, Becker IC et al. Efficient megakaryopoiesis and platelet production require phospholipid remodeling and PUFA uptake through CD36. Nat Cardiovasc Res 2023;2(8):746-763.
63 Alattar AG, Storry JR, Olsson ML. Evidence that CD36 is expressed on red blood cells and constitutes a novel blood group system of clinical importance. Vox Sang 2024;119(5):496-504.
64 Weiss G, Ganz T, Goodnough LT. Anemia of inflammation. Blood 2019;133(1):40-50.
65 Hess SY, Owais A, Jefferds MED et al. Accelerating action to reduce anemia: Review of causes and risk factors and related data needs. Ann N Y Acad Sci 2023;1523(1):11-23.
66 Lewis R, Bewersdorf JP, Zeidan AM. Clinical Management of Anemia in Patients with Myelodysplastic Syndromes: An Update on Emerging Therapeutic Options. Cancer Manag Res 2021;13:645-657.
67 Garcia-Manero G, Santini V, Almeida A et al. Phase III, Randomized, Placebo-Controlled Trial of CC-486 (Oral Azacitidine) in Patients With Lower-Risk Myelodysplastic Syndromes. J Clin Oncol 2021;39(13):1426-1436.

## Figure Legends

**Figure 1: Epo induces high expression of CD105 and CD71 in human BM *ex vivo* cultures.** BM $CD34^+$ HSPCs were cultured in medium containing or lacking Epo. Surface expression of CD105 and CD71 was examined by flow cytometry, and percentages of positive cells within $LiveLin^-CD123^-$ cells are shown. **(A)** Overall expression and **(B)** representative plots for CD71 expression. Gates for low and high expression as determined by anti-CD71/FITC antibody staining are shown. **(C)** Percentages of $CD71^{hi}$ (top) and $CD71^{lo}$ (bottom) cells in each condition. **(D)** Overall expression and **(E)** representative scatter plots for CD105 expression. Gates for low and high expression as determined by anti-CD105/PE antibody staining are shown. **(F)** Percentages of $CD105^{hi}$ (top) and $CD105^{lo}$ (bottom) cells in each condition. P-values ≤ 0.05 were considered significant; *$p < 0.05$, **$p < 0.01$, ***$p < 0.001$ (n = 5). Abbreviations: Epo; erythropoietin, Lin; lineage markers, including CD3, CD10, CD11b, CD19, CD41.

**Figure 2: Immunophenotyping strategy for Epo-dependent resolution of EE populations.** Cells from *ex vivo* cultures of BM $CD34^+$ HSPCs incubated in medium containing or lacking Epo were analyzed on days 4, 7, and 10 for the indicated surface markers by flow cytometry (Panel 1 in Table S2). **(A)** Representative scatter plots from the analysis of EE populations in +Epo cultures on day 4. $CD235a^-CD71^+$ cells are gated from $LiveLin^-CD123^-$ cells (i), then $CD117^+CD49d^+$ cells are selected (ii), and $CD105^+$ cells are stratified based on CD34 expression (iii)—all $CD34^+CD105^+$ cells are considered BFU-E and all $CD34^-CD105^+$ cells are considered CFU-E. BFU-E and CFU-E were further stratified based on CD71 and CD105. BFU-E showed two populations: $CD71^{lo}CD105^{lo}$ (earlyB) and $CD71^{hi}CD105^{lo}$ (lateB) (iv). Within CFU-E, three populations were observed: $CD71^{lo}CD105^{lo}$ (earlyC), $CD71^{hi}CD105^{lo}$ (midC), and $CD71^{hi}CD105^{hi}$ (lateC) (v). **(B)** Representative scatter plots for analysis of EE populations in cultures lacking Epo on day 4 by the same strategy as in (A). Comparison of percentage of erythroid progenitor and erythroblast populations in BM HSPC cultures: **(C)** total BFU-E ($CD34^+CD105^+$) as a percentage of $CD49d^+CD117^+$ cells, **(D)** earlyB ($CD34^+CD71^{lo}CD105^{lo}$) and **(E)** lateB ($CD34^+CD71^{hi}CD105^{lo}$) as a percentage of total BFU-E; **(F)** total CFU-E ($CD34^-CD105^+$) as a percentage of $CD49d^+CD117^+$ cells; **(G)** ProE ($CD105^{hi}CD235a^{lo}$) and early BasoE ($CD105^{hi}CD235a^{hi}$) and **(H)** late BasoE ($CD105^{med}CD235a^{hi}$), PolyE ($CD105^{lo}CD235a^{hi}$), and OrthoE ($CD105^-CD235a^{hi}$) as a percentage of $LiveLin^-CD123^-$ cells; **(I)** earlyC ($CD34^-CD71^{lo}CD105^{lo}$), **(J)** midC ($CD34^-CD71^{hi}CD105^{lo}$), and **(K)** lateC ($CD34^-CD71^{hi}CD105^{hi}$) as a percentage of total CFU-E. P-values ≤ 0.05 were considered significant (*$p < 0.05$, **$p < 0.01$, ***$p < 0.001$; n = 8 for EE populations; n = 6 for erythroblast populations). Abbreviations: Epo; erythropoietin, BFU-E; burst forming unit-erythroid, CFU-E; colony forming unit-erythroid, earlyB; early BFU-E, lateB; late BFU-E, earlyC; early CFU-E, midC; mid CFU-E, lateC; late CFU-E, ProE; proerythroblast, BasoE; basophilic erythroblast, PolyE; polychromatic erythroblast, OrthoE; orthochromatic erythroblast, Lin; lineage markers, including CD3, CD10, CD11b, CD19, CD41.

**Figure 3. CD36 expression within EE populations reveals two potential differentiation routes.** Cells from *ex vivo* cultures of BM $CD34^+$ HSPCs incubated in medium containing or lacking Epo were analyzed for expression of CD36 within all five EE subpopulations by flow cytometry. Representative scatter plots from day 4 analysis of cells cultured **(A)** with and **(B)** without Epo, depicting CD36 expression within each of the five EE populations—i) earlyB, ii) lateB, iii) earlyC, iv) midC, and v) lateC. **(C)** Quantification of CD36 expression in all five EE populations on day 4 of culture in medium containing Epo (n = 5). Bar graphs for day 7 and 10 are shown in Figure S3. **(D)** Proposed differentiation routes for the transition of progenitors in EE. Abbreviations: Epo; erythropoietin, BFU-E; burst forming unit-erythroid, CFU-E; colony

forming unit-erythroid, earlyB; early BFU-E, lateB; late BFU-E, earlyC; early CFU-E, midC; mid CFU-E, lateC; late CFU-E.

**Figure 4. Prospective analysis resolves all five EE populations in human BM.** BM cells were thawed, stimulated overnight in medium lacking Epo (see Materials and Methods), then analyzed using the same immunophenotyping strategy as in Figure 2A. **(A)** EarlyB and lateB populations in BM-derived $CD34^+$ HSPCs. **(B)** EE populations in BM-derived MNCs. $CD235a^-CD71^+$ cells are gated from $LiveLin^-CD123^-$ cells, then $CD117^+CD49d^+$ cells are selected, and $CD105^+$ cells are stratified based on CD34 expression—all $CD34^+CD105^+$ cells are considered BFU-E, and all $CD34^-CD105^+$ cells are considered CFU-E. BFU-E and CFU-E were further stratified based on CD71 and CD105. BFU-E showed two populations: $CD71^{lo}CD105^{lo}$ (earlyB) and $CD71^{hi}CD105^{lo}$ (lateB). Within CFU-E, three populations were observed: $CD71^{lo}CD105^{lo}$ (earlyC), $CD71^{hi}CD105^{lo}$ (midC), and $CD71^{hi}CD105^{hi}$ (lateC). Abbreviations: MNC; mononuclear cells, Lin; lineage markers, including CD3, CD10, CD11b, CD19, CD41.

**Figure 5. Sorted EE populations differentiate via the expected trajectories and enter TED.** Cells from *ex vivo* cultures of BM-derived $CD34^+$ HSPCs were incubated in complete medium containing Epo. EE populations were isolated by FACS on day 4, recultured in suspension, and analyzed using the strategies described in Figure 2A (EE) and by Yan et al. 2021 [22] (TED). Representative scatter plots for BFU-E, CFU-E, and erythroblast subpopulations arising from cultures of sorted (**A**) earlyB, (**B**) lateB, (**C**) earlyC/midC mix, and (**D**) lateC on days 4 and 7 of reculture. Abbreviations: BFU-E; burst-forming unit erythroid, CFU-E; colony-forming unit erythroid, ProE; proerythroblast, BasoE; basophilic erythroblast, PolyE; polychromatic erythroblast, OrthoE; orthochromatic erythroblast.

**Figure 6. Colony forming potential of sorted EE populations.** Cells from *ex vivo* cultures of BM-derived $CD34^+$ HSPCs were incubated in complete medium containing Epo. EE populations were isolated by FACS on day 4 according to the strategy in Figure 2A, then replated in methylcellulose containing SCF, IL-3, GM-CSF, and Epo or Epo only. All colonies were counted on day 14 and normalized to 10,000 cells. Representative images of CFU-GM, large BFU-E, small BFU-E, and CFU-E colonies at (**A**) 40x and (**B**) 100x magnification. Quantification of colonies formed by sorted (**C**) earlyB, (**D**) lateB, (**E**) earlyC/midC mix, and (**F**) lateC (n = 3). EE cells were also sorted based off CD36 expression within total BFU-E ($CD34^+CD105^+$) and total CFU-E ($CD34^-CD105^+$) (Figure 2A iii) to generate four populations: $CD36^+$-BFU-E, $CD36^-$-BFU-E, $CD36^+$-CFU-E, and $CD36^-$-CFU-E. Quantification of colony formation for each population is shown for **(G)** complete medium and **(H)** Epo only medium (n = 2). Abbreviations: Epo; erythropoietin, CFU-GEMM; colony forming unit-granulocyte, erythrocyte, monocyte, megakaryocyte, CFU-GM; colony forming unit-granulocyte monocyte, BFU-E; burst-forming unit erythroid, CFU-E; colony-forming unit erythroid.

**Figure 7. Occurrence of EE subtypes and Epo-dependence of lateC formation in CB-derived $CD34^+$ HSPC cultures.** Cells from *ex vivo* cultures of CB-derived $CD34^+$ HSPCs incubated in medium containing or lacking Epo were analyzed on days 4, 7, and 10 using the immunophenotyping strategy described in Figure 2A. $CD235a^-CD71^+$ cells are gated from $LiveLin^-CD123^-$ cells (i), then $CD117^+CD49d^+$ cells are selected (ii), and $CD105^+$ cells are stratified based on CD34 expression (iii)—all $CD34^+CD105^+$ cells are considered BFU-E, and all $CD34^-CD105^+$ cells are considered CFU-E. BFU-E and CFU-E were further stratified based on CD71 and CD105. BFU-E showed two populations: $CD71^{lo}CD105^{lo}$ (earlyB) and $CD71^{hi}CD105^{lo}$ (lateB) (iv). Within CFU-E, three populations were observed: $CD71^{lo}CD105^{lo}$ (earlyC), $CD71^{hi}CD105^{lo}$ (midC), and $CD71^{hi}CD105^{hi}$ (lateC) (v). Representative scatter plots from day 7

of analysis for cells cultured in medium **(A)** with and **(B)** without Epo. Comparison of percentage of CFU-E subpopulations in CB HSPC cultures: **(C)** earlyC ($CD34^{-}CD71^{lo}CD105^{lo}$), **(D)** midC ($CD34^{-}CD71^{hi}CD105^{lo}$), and **(E)** lateC ($CD34^{-}CD71^{hi}CD105^{hi}$) are all depicted as a percentage of total CFU-E. P-values ≤ 0.05 were considered significant (*p < 0.05, **p < 0.01; n = 4). **(F)** Schematic representation of the two routes to formation of lateC. One passes through the earlyC stage, whereas the other bypasses earlyC due to direct conversion of lateB to midC. EarlyB to lateB and earlyC to midC transitions are accompanied by an increase in the expression of CD71 and gain of CD36 positivity, whereas earlyB to earlyC and lateB to midC transitions are accompanied by the loss of CD34 positivity. Both paths converge at midC, which require Epo to transition to lateC, characterized as $CD34^{-}CD71^{hi}CD105^{hi}$ within the $CD235a^{-}$ compartment. Abbreviations: Epo; erythropoietin, BFU-E; burst-forming unit erythroid, CFU-E; colony-forming unit erythroid, earlyB; early BFU-E, lateB; late BFU-E, earlyC; early CFU-E, midC; mid CFU-E, lateC; late CFU-E, Lin; lineage markers, including CD3, CD10, CD11b, CD19, CD41.

**Figure S1. Epo-dependence of TED during *ex vivo* culture of human BM-derived HSPCs.** Cells from cultures of BM $CD34^{+}$ HSPCs in medium containing or lacking Epo were analyzed for surface expression of markers by flow cytometry, and percentages are shown for days 4, 7, and 10 of culture. **(A)** Representative scatter plots and **(B)** quantification of CD235a expression within $LiveLin^{-}CD123^{-}$ cells. **(C)** Representative scatter plots of erythroblast populations using the flow cytometry strategy developed by Yan et al., 2021 [22]. No erythroblast populations are observed in −Epo cultures. P-values ≤ 0.05 were considered significant; *p < 0.05, **p < 0.01, ***p < 0.001 (n = 3). Abbreviations: ProE; proerythroblast, BasoE; basophilic erythroblast, PolyE; polychromatic erythroblast, OrthoE; orthochromatic erythroblast, Epo; erythropoietin, Lin: lineage markers, including CD3, CD10, CD11b, CD19, CD41.

**Figure S2. Analysis of surface markers on cells from *ex vivo* cultures of human BM-derived HSPCs.** Cells from cultures of BM $CD34^{+}$ HSPCs in medium containing or lacking Epo were analyzed for surface expression of markers by flow cytometry. All results are shown as percentages within $LiveLin^{-}CD123^{-}$ cells for days 4, 7, and 10 of culture. **(A)** Quantification and **(B)** representative scatter plots for $CD49d^{+}$ cells. **(C)** Quantification and **(D)** representative scatter plots for $CD117^{+}$ cells. **(E)** Quantification and **(F)** representative scatter plots for $CD36^{+}$ cells. P-values ≤ 0.05 were considered significant; *p < 0.05 (n = 5). Abbreviations: Epo; erythropoietin, Lin; lineage markers, including CD3, CD10, CD11b, CD19, CD41.

**Figure S3. CD36 expression within early erythroid populations.** Cells from *ex vivo* cultures of BM $CD34^{+}$ HSPCs incubated in medium containing or lacking Epo were analyzed on days 4, 7, and 10 of culture using the strategy in Figure 2A. CD36 expression was then assessed within each EE subpopulation. Bar graphs depicting CD36 expression in all five EE populations on days **(A)** 7 and **(B)** 10 from cultures containing Epo. Quantification for day 4 is shown in Figure 3. Line graphs indicate $CD36^{+}$ cells within **(C)** earlyB, **(D)** lateB, **(E)** earlyC, **(F)** midC, and **(G)** lateC in both conditions. P-values ≤ 0.05 were considered significant; n = 5. Abbreviations: Epo; erythropoietin, BFU-E; burst-forming unit erythroid, CFU-E; colony-forming unit erythroid, earlyB; early BFU-E, lateB; late BFU-E, earlyC; early CFU-E, midC; mid CFU-E, lateC; late CFU-E, Lin; lineage markers, including CD3, CD10, CD11b, CD19, CD41.

**Figure S4. Flow cytometry analysis of BFU-E and CFU-E populations using an alternative antibody panel.** Cells from *ex vivo* cultures of BM $CD34^{+}$ HSPCs incubated in medium containing or lacking Epo were analyzed for the indicated surface markers by flow cytometry (Panel 2 in Table S2). In this analysis, CD105, CD71, CD36, and CD49d were stained with BV421, APC, FITC, and PE labeled antibodies, respectively. **(A)** Representative scatter plots for

**(A)** $CD105^+$ and **(B)** $CD71^+$ cells within the $LiveLin^-CD123^-$ compartment. Cells exhibiting low and high expression are indicated. **(C)** Representative scatter plots for the analysis of EE populations in +Epo cultures. $CD235a^-CD71^+$ cells are gated from $LiveLin^-CD123^-$ cells (i), then $CD117^+CD49d^+$ cells are selected (ii), and $CD105^+$ cells are stratified based on CD34 expression (iii)—all $CD34^+CD105^+$ cells are considered BFU-E and all $CD34^-CD105^+$ cells are considered CFU-E. BFU-E and CFU-E were further stratified based on CD71 and CD105. BFU-E showed two populations: $CD71^{lo}CD105^{lo}$ (earlyB) and $CD71^{hi}CD105^{lo}$ (lateB) (iv). Within CFU-E, three populations were observed: $CD71^{lo}CD105^{lo}$ (earlyC), $CD71^{hi}CD105^{lo}$ (midC), and $CD71^{hi}CD105^{hi}$ (lateC) (v). **(D)** Representative scatter plots for the analysis of populations in cultures lacking Epo by the same strategy as in (C). Representative scatter plots from day 4 depicting CD36 expression within each of the five EE populations—i) earlyB, ii) lateB, iii) earlyC, iv) midC, and v) lateC—for cells cultured **(E)** with and **(F)** without Epo. Abbreviations: Epo; erythropoietin, BFU-E; burst-forming unit erythroid, CFU-E; colony-forming unit erythroid, Lin; lineage markers, including CD3, CD10, CD11b, CD19, CD41.

**Figure S5. Analysis of Epo-dependent formation of lateC using antibodies labeled with alternative fluorophores.** Cells from *ex vivo* cultures of BM $CD34^+$ HSPCs incubated in medium containing or lacking Epo were analyzed by flow cytometry on days 4, 7, and 10 of culture (Panel 2 in Table S2). Bar graphs indicate percentage of **(A)** total BFU-E and **(B)** total CFU-E within $CD49d^+CD117^+$ cells, **(C)** earlyB and **(D)** lateB within total BFU-E, and **(E)** earlyC, **(F)** midC, and **(G)** lateC within total CFU-E. P-values ≤ 0.05 were considered significant (*$p < 0.05$, **$p < 0.01$; n = 3). Abbreviations: Epo; erythropoietin, BFU-E; burst-forming unit erythroid, CFU-E; colony-forming unit erythroid, earlyB; early BFU-E, lateB; late BFU-E, earlyC; early CFU-E, midC; mid CFU-E, lateC; late CFU-E.

**Figure S6. Assessment of early erythroid progenitors using published immunophenotyping strategies** Cells from *ex vivo* cultures of BM $CD34^+$ HSPCs incubated in medium containing or lacking Epo were analyzed for the indicated surface markers by flow cytometry. **(A)** Analysis of EE progenitors on day 4 using the strategy described by Li et al., 2014 [23]. Briefly, $CD235a^-$ cells are selected from $LiveLin^-CD123^-$ cells and then stratified based on CD36 expression. $CD36^-$ cells were evaluated for CD34 expression, and $CD36^-CD34^+$ cells were considered BFU-E. $CD36^+$ cells are evaluated for CD71 expression, and $CD36^+CD71^+$ cells were considered CFU-E. **(B)** Assessment of EE progenitors on day 7 using the immunophenotyping strategy described by Yan et al., 2021 [22]. Briefly, $CD117^+$ cells were gated from $LiveCD235a^-$ cells, then $CD45RA^-CD41^-$ cells were selected and assessed for CD123 and CD71 expression. $CD123^-CD71^+$ cells are then stratified based on the expression of CD34 and CD105. Abbreviations: Epo; erythropoietin, Lin; lineage markers, including CD3, CD10, CD11b, CD19, CD41.

**Figure S7. Proliferation of sorted EE populations and validation of colony forming potential of hematopoietic cultures. (A)** Cells from *ex vivo* cultures of BM-derived $CD34^+$ HSPCs were incubated in complete medium containing Epo. On day 4, EE populations were isolated by FACS according to the strategy in Figure 2A, then replated in suspension in complete medium containing Epo. Quantification of cell proliferation for each of the sorted populations (earlyC and midC sorted together) is shown (n = 4 or 5). On the graph, day 1 corresponds to sorting/reculturing day. **(B)** Cells from *ex vivo* cultures of BM-derived $CD34^+$ HSPCs were incubated in +Epo medium. Whole cell suspensions were collected on day 4 and plated in methylcellulose under four conditions: complete medium (MethoCult® classic containing SCF, IL-3, GM-CSF, and Epo), complete medium without Epo, Epo only, or no cytokines. Quantification of colonies (CFU-GEMM, CFU-GM, large BFU-E, small BFU-E, and CFU-E) counted 14 days post-plating is shown (n = 3). CFU-GM colonies were observed in

complete medium and complete medium without Epo. Large and small BFU-E colonies were observed only in complete medium. CFU-E colonies were formed in complete medium and Epo only medium. No colonies formed in medium lacking cytokines. Colony counts are normalized to 10,000 cells. Abbreviations: Epo; erythropoietin, CFU-GEMM; colony forming unit-granulocyte, erythrocyte, monocyte, megakaryocyte, CFU-GM; colony forming unit-granulocyte monocyte, BFU-E; burst-forming unit erythroid, CFU-E; colony-forming unit erythroid.

**Figure S8. Epo-dependence of TED during *ex vivo* culture of human CB-derived HSPCs.** Cells from cultures of CB $CD34^+$ HSPCs in medium containing or lacking Epo were analyzed for surface expression of markers by flow cytometry, and percentages are shown for days 4, 7, and 10 of culture. **(A)** Representative scatter plots and **(B)** quantification of CD235a expression as a percentage of $LiveLin^-CD123^-$ cells. **(C)** Representative scatter plots of erythroblast in cultures with and without Epo using the flow cytometry strategy developed by Yan et al., 2021 [22]. No erythroblast populations are observed in −Epo cultures. P-values ≤ 0.05 were considered significant; *p < 0.05, **p < 0.01, ***p < 0.001, **** p < 0.0001 (n = 4). Abbreviations: ProE; proerythroblast, BasoE; basophilic erythroblast, PolyE; polychromatic erythroblast, OrthoE; orthochromatic erythroblast, Epo; erythropoietin, Lin; lineage markers, including CD3, CD10, CD11b, CD19, CD41.

**Figure S9: Epo induces high expression of CD105 and CD71 in human CB *ex vivo* cultures.** CB $CD34^+$ HSPCs were cultured in medium containing or lacking Epo. Surface expression of CD105 and CD71 was determined by flow cytometry, and percentages of positive cells within the $LiveLin^-CD123^-$ compartment are shown. **(A)** Quantification and **(B)** representative plots for CD71 expression. Gates for low and high expression as determined by anti-CD71/FITC antibody staining are shown. **(C)** Comparison of percentage of $CD71^{hi}$ (top) and $CD71^{lo}$ (bottom) cells in both conditions. **(D)** Quantification and **(E)** representative scatter plots for CD105 expression. Gates for low and high expression as determined by anti-CD105/PE antibody staining are shown. **(F)** Comparison of percentage of $CD105^{hi}$ (top) and $CD105^{lo}$ (bottom) cells in both conditions. P-values ≤ 0.05 were considered significant; *p < 0.05, **p < 0.01, ***p < 0.001, **** p < 0.0001 (n = 4). Abbreviations: Epo; erythropoietin, Lin; lineage markers, including CD3, CD10, CD11b, CD19, CD41.

**Figure S10. Epo-dependence of EE surface markers during *ex vivo* culture of human CB-derived HSPCs.** Cells from cultures of CB $CD34^+$ HSPCs in medium containing or lacking Epo were analyzed for surface expression of markers by flow cytometry. All results are shown as percentages within $LiveLin^-CD123^-$ cells for days 4, 7, and 10 of culture. **(A)** Quantification and **(B)** representative scatter plots depicting $CD49d^+$ cells. **(C)** Quantification and **(D)** representative scatter plots depicting $CD117^+$ cells. **(E)** Quantification and **(F)** representative scatter plots depicting $CD36^+$ cells. P-values ≤ 0.05 were considered significant; *p < 0.05, **p < 0.01, ***p < 0.001, **** p < 0.0001 (n = 4). Abbreviations: Epo; erythropoietin, Lin; lineage markers, including CD3, CD10, CD11b, CD19, CD41.

**Figure S11. Epo-dependence of lateC formation is observed in cultures from CB-derived $CD34^+$ HSPCs.** Cells from *ex vivo* cultures of CB-derived $CD34^+$ HSPCs incubated in medium containing or lacking Epo were analyzed on days 4, 7, and 10 using the immunophenotyping strategy described in Figure 2A. Representative scatter plots from the analysis of EE populations on day 4 in cultures **(A)** containing and **(B)** lacking Epo. $CD235a^-CD71^+$ cells are gated from $LiveLin^-CD123^-$ cells (i), then $CD117^+CD49d^+$ cells are selected (ii), and $CD105^+$ cells are stratified based on CD34 expression (iii)—all $CD34^+CD105^+$ cells are considered BFU-E, and all $CD34^-CD105^+$ cells are considered CFU-E. BFU-E and CFU-E were further stratified

based on CD71 and CD105. BFU-E showed two populations: $CD71^{lo}CD105^{lo}$ (earlyB) and $CD71^{hi}CD105^{lo}$ (lateB) (iv). Within CFU-E, three populations were observed: $CD71^{lo}CD105^{lo}$ (earlyC), $CD71^{hi}CD105^{lo}$ (midC), and $CD71^{hi}CD105^{hi}$ (lateC) (v). Comparison of percentage of erythroid progenitor populations in CB HSPC cultures: **(C)** total BFU-E ($CD34^{+}CD105^{+}$) and **(D)** total CFU-E ($CD34^{-}CD105^{+}$) are depicted as a percentage of $CD49d^{+}CD117^{+}$ cells, **(E)** earlyB ($CD34^{+}CD71^{lo}CD105^{lo}$) and **(F)** lateB ($CD34^{+}CD71^{hi}CD105^{lo}$) are depicted as a percentage of total BFU-E. P-values ≤ 0.05 were considered significant (n = 4). Abbreviations: Epo; erythropoietin, BFU-E; burst-forming unit erythroid, CFU-E; colony-forming unit erythroid, earlyB; early BFU-E, lateB; late BFU-E, Lin; lineage markers, including CD3, CD10, CD11b, CD19, CD41.

**Figure S12. CD36 expression within EE populations in CB-derived *ex vivo* cultures.** Cells from *ex vivo* cultures of CB $CD34^{+}$ HSPCs were analyzed on days 4, 7, and 10 for expression of CD36 within all five EE subpopulations by flow cytometry. Representative scatter plots from day 4 of culture depicting CD36 expression within each of the five EE populations—i) earlyB, ii) lateB, iii) earlyC, iv) midC, and v) lateC in medium **(A)** with and **(B)** without Epo. Quantification of CD36 expression in all five EE populations on **(C)** day 4, **(D)** day 7, and **(E)** day 10 in medium containing Epo. Line graphs indicate $CD36^{+}$ cells within **(F)** earlyB, **(G)** lateB, **(H)** earlyC, **(I)** midC, and **(J)** lateC in both conditions. P-values ≤ 0.05 were considered significant; n = 4. Abbreviations: Epo; erythropoietin, BFU-E; burst forming unit-erythroid, CFU-E; colony forming unit-erythroid, earlyB; early BFU-E, lateB; late BFU-E, earlyC; early CFU-E, midC; mid CFU-E, lateC; late CFU-E.

**Figure S13. Comparison of EE populations in CB- and BM-derived *ex vivo* cultures.** Cells from *ex vivo* cultures of CB and BM $CD34^{+}$ HSPCs incubated in complete medium containing Epo were analyzed on days 4, 7, and 10 for expression of indicated markers, all five EE populations, and CD36 expression within them. Line graphs comparing expression of **(A)** CD235a, **(B)** CD49d, **(C)** CD117, **(D)** CD36, **(E)** $CD71^{hi}$, **(F)** $CD71^{lo}$, **(G)** CD71, **(H)** $CD105^{hi}$, **(I)** $CD105^{lo}$, and **(J)** CD105 as a percent of $LiveLin^{-}CD123^{-}$ cells. Line graphs comparing formation of **(K)** earlyB and **(L)** lateB as percentage of total BFU-E and of **(M)** earlyC, **(N)** midC, and **(O)** lateC as a percentage of total CFU-E. Line graphs comparing expression of CD36 within **(P)** earlyB, **(Q)** lateB, **(R)** earlyC, **(S)** midC, and **(T)** lateC. (n = 3 CB and BM samples). Abbreviations: Epo; erythropoietin, earlyB; early BFU-E, lateB; late BFU-E, earlyC; early CFU-E, midC; mid CFU-E, lateC; late CFU-E, Lin; lineage markers, including CD3, CD10, CD11b, CD19, CD41.

**Figure S14. Comparison of TED populations in CB- and BM-derived *ex vivo* cultures.** Cells from *ex vivo* cultures of CB and BM $CD34^{+}$ HSPCs incubated in complete medium containing Epo were analyzed on days 4, 7, and 10 for erythroblast populations according to the flow cytometry strategy developed by Yan et al., 2021 [22]. Line graphs comparing expression of **(A)** ProE, **(B)** early BasoE, **(C)** late BasoE, **(D)** PolyE, and **(E)** OrthoE as a percentage of $LiveLin^{-}CD123^{-}$ cells. P-values ≤ 0.05 were considered significant; *$p < 0.05$ (n = 3 CB and 3 BM samples for all). Abbreviations: Epo; erythropoietin, ProE; proerythroblast, BasoE; basophilic erythroblast, PolyE; polychromatic erythroblast, OrthoE; orthochromatic erythroblast, Lin; lineage markers, including CD3, CD10, CD11b, CD19, CD41.

Figure 1

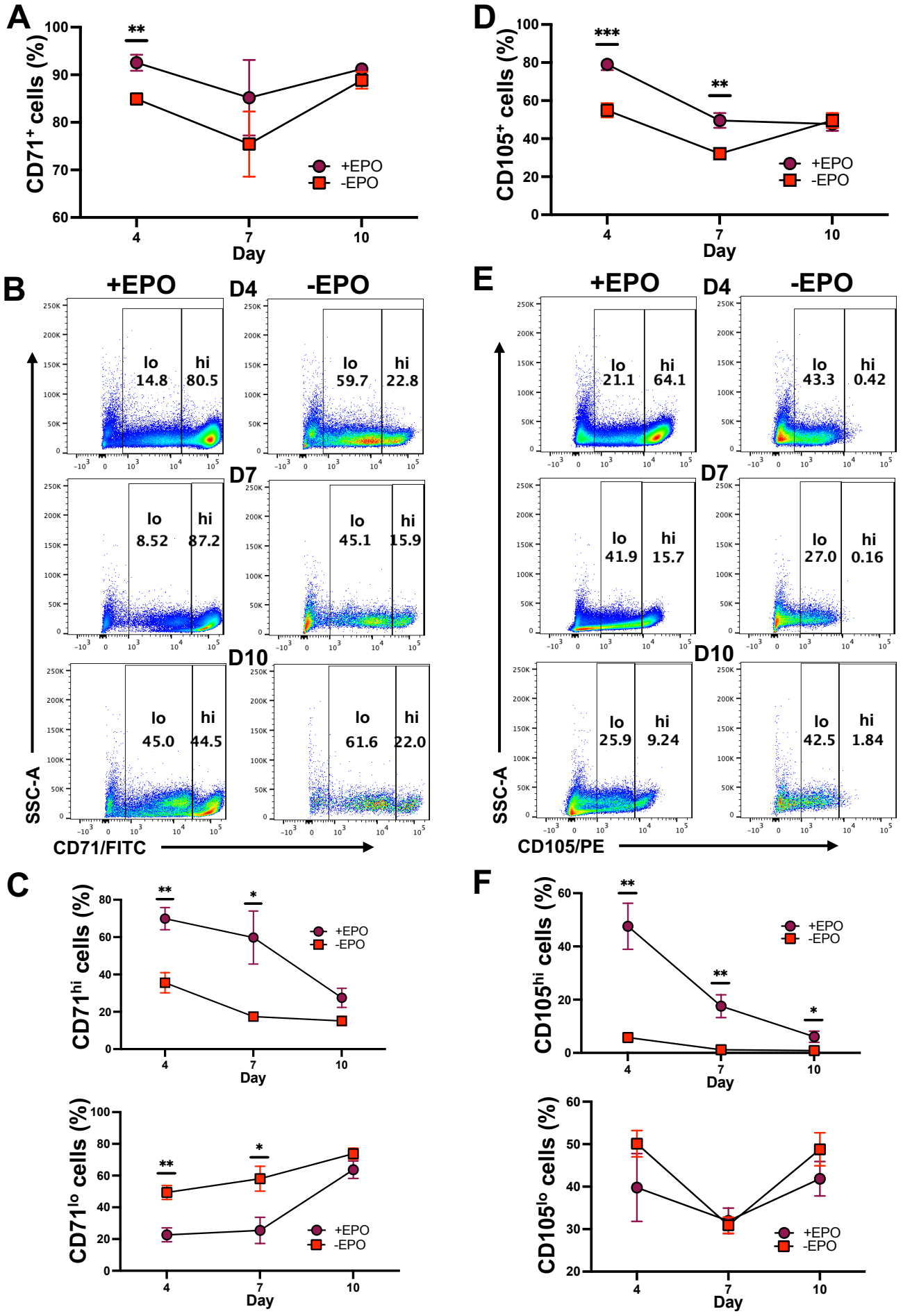
A
CD71+ cells (%)
Day
+EPO
-EPO
D
CD105+ cells (%)
Day
+EPO
-EPO
B
+EPO
D4
-EPO
D7
D10
lo 14.8
hi 80.5
lo 59.7
hi 22.8
lo 8.52
hi 87.2
lo 45.1
hi 15.9
lo 45.0
hi 44.5
lo 61.6
hi 22.0
SSC-A
CD71/FITC
E
+EPO
D4
-EPO
D7
D10
lo 21.1
hi 64.1
lo 43.3
hi 0.42
lo 41.9
hi 15.7
lo 27.0
hi 0.16
lo 25.9
hi 9.24
lo 42.5
hi 1.84
SSC-A
CD105/PE
C
CD71hi cells (%)
CD71lo cells (%)
Day
+EPO
-EPO
F
CD105hi cells (%)
CD105lo cells (%)
Day
+EPO
-EPO

Figure 2

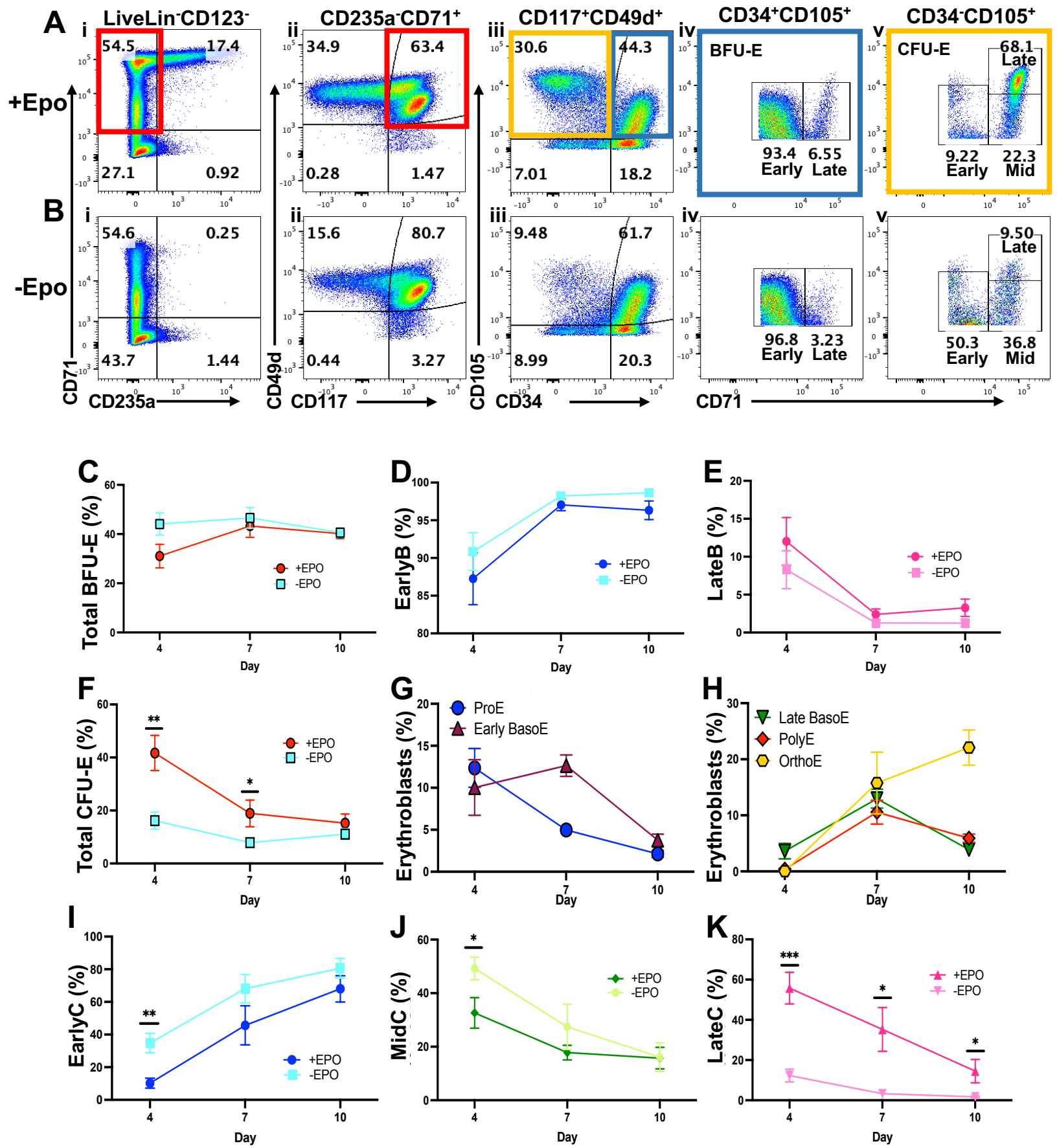
A
B
i
ii
iii
iv
v
LiveLin-CD123-
CD235a-CD71+
CD117+CD49d+
CD34+CD105+
CD34-CD105+
+Epo
-Epo
54.5
17.4
27.1
0.92
34.9
63.4
0.28
1.47
30.6
44.3
7.01
18.2
BFU-E
93.4
6.55
Early
Late
CFU-E
68.1
Late
9.22
22.3
Early
Mid
54.6
0.25
43.7
1.44
15.6
80.7
0.44
3.27
9.48
61.7
8.99
20.3
96.8
3.23
Early
Late
9.50
Late
50.3
36.8
Early
Mid
CD71
CD235a
CD49d
CD117
CD105
CD34
CD71
C
Total BFU-E (%)
Day
+EPO
-EPO
D
EarlyB (%)
E
LateB (%)
F
Total CFU-E (%)
**
*
G
Erythroblasts (%)
ProE
Early BasoE
H
Late BasoE
PolyE
OrthoE
I
EarlyC (%)
J
MidC (%)
K
LateC (%)
***

Figure 3

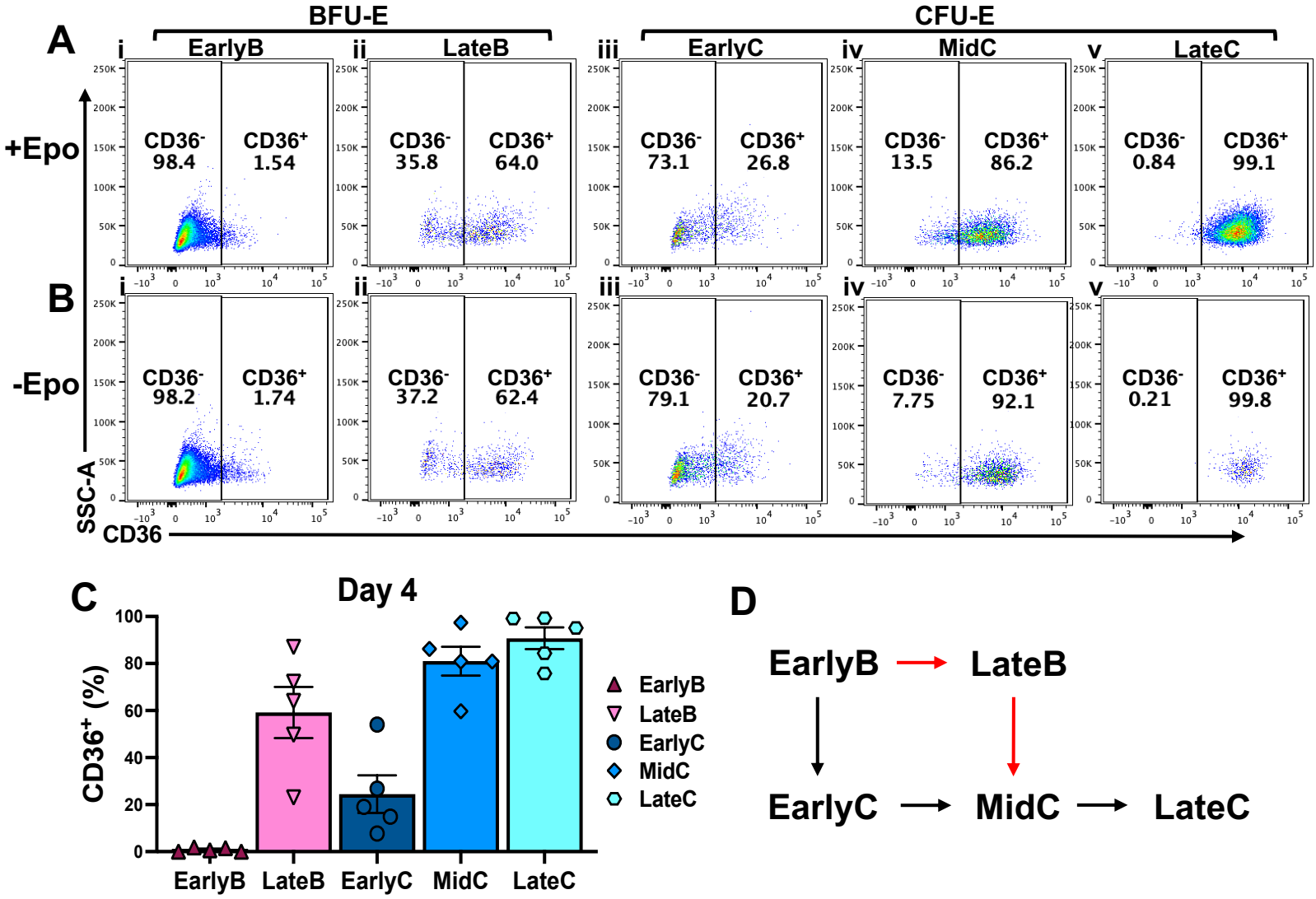
A
BFU-E
CFU-E
i EarlyB
ii LateB
iii EarlyC
iv MidC
v LateC
+Epo
CD36- 98.4
CD36+ 1.54
CD36- 35.8
CD36+ 64.0
CD36- 73.1
CD36+ 26.8
CD36- 13.5
CD36+ 86.2
CD36- 0.84
CD36+ 99.1
B
-Epo
CD36- 98.2
CD36+ 1.74
CD36- 37.2
CD36+ 62.4
CD36- 79.1
CD36+ 20.7
CD36- 7.75
CD36+ 92.1
CD36- 0.21
CD36+ 99.8
SSC-A
CD36
C
Day 4
CD36+ (%)
EarlyB
LateB
EarlyC
MidC
LateC
D
EarlyB
LateB
EarlyC
MidC
LateC

Figure 4

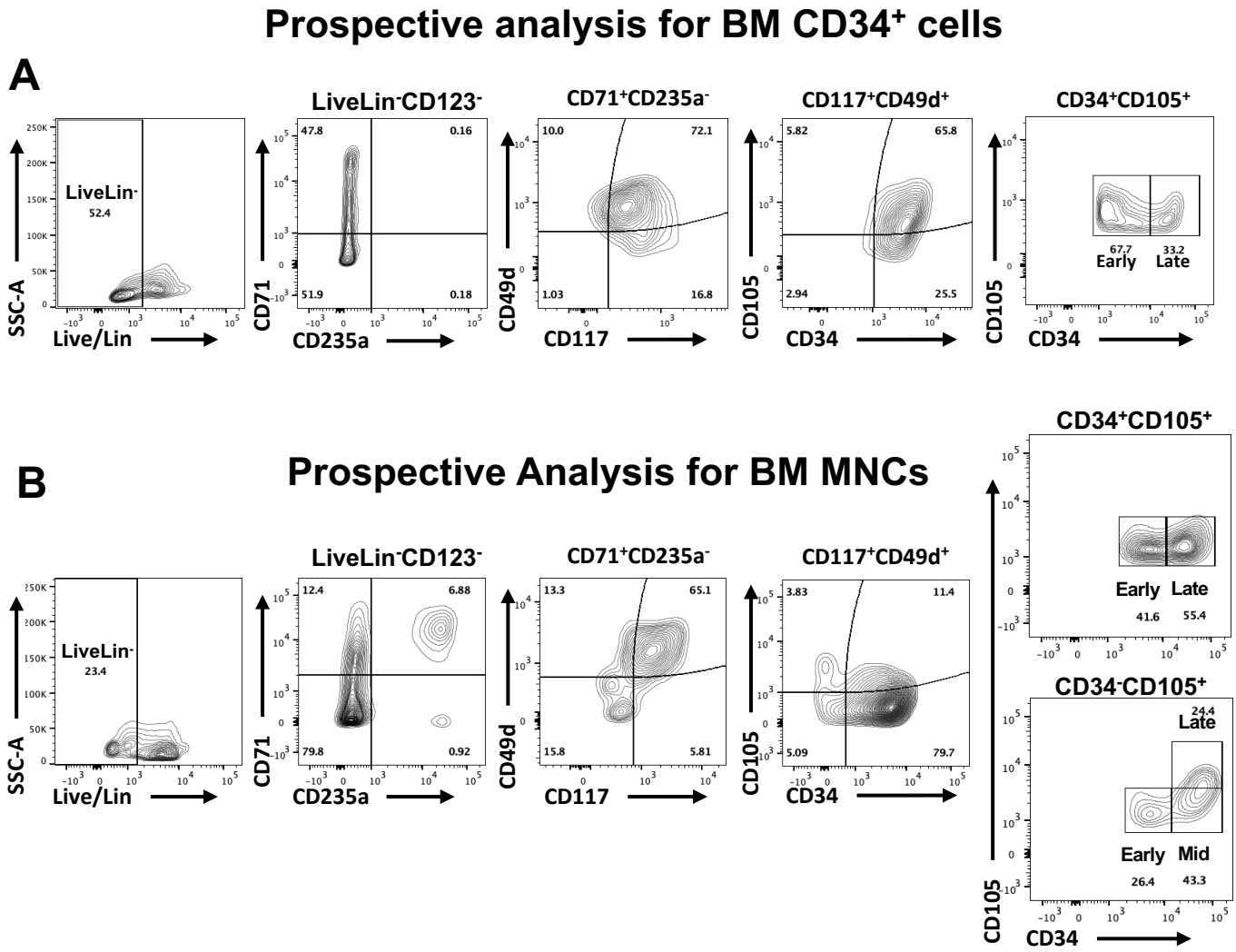
Prospective analysis for BM CD34+ cells
A
LiveLin-CD123-
CD71+CD235a-
CD117+CD49d+
CD34+CD105+
LiveLin-
52.4
SSC-A
Live/Lin
47.8
0.16
51.9
0.18
CD71
CD235a
10.0
72.1
1.03
16.8
CD49d
CD117
5.82
65.8
2.94
25.5
CD105
CD34
67.7
Early
33.2
Late
CD105
CD34
B
Prospective Analysis for BM MNCs
LiveLin-CD123-
CD71+CD235a-
CD117+CD49d+
CD34+CD105+
LiveLin-
23.4
SSC-A
Live/Lin
12.4
6.88
79.8
0.92
CD71
CD235a
13.3
65.1
15.8
5.81
CD49d
CD117
3.83
11.4
5.09
79.7
CD105
CD34
Early
Late
41.6
55.4
CD34-CD105+
24.4
Late
Early
Mid
26.4
43.3
CD105
CD34

# Figure 5

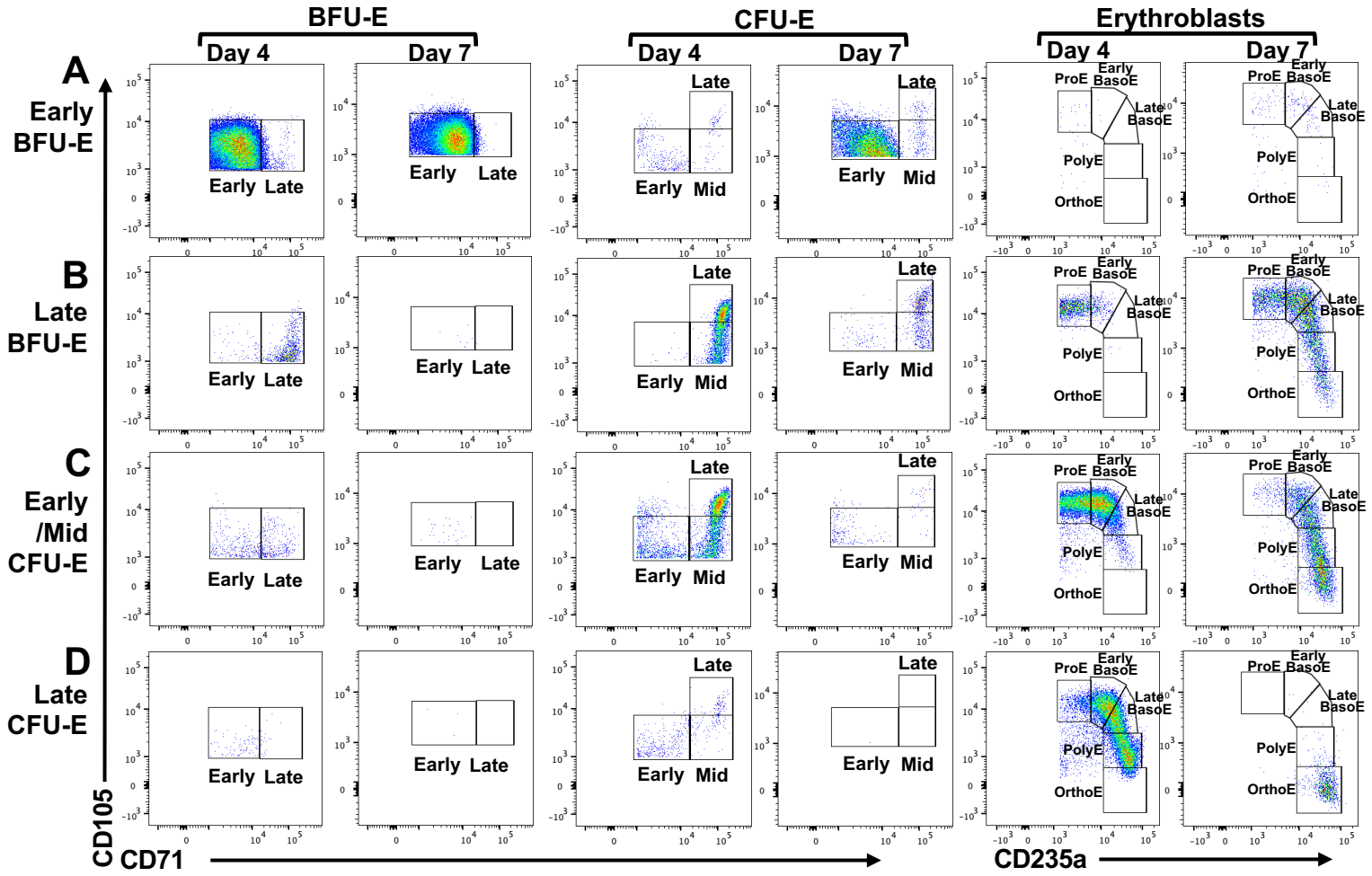
BFU-E
CFU-E
Erythroblasts
Day 4
Day 7
A
Early BFU-E
B
Late BFU-E
C
Early /Mid CFU-E
D
Late CFU-E
Early
Late
Mid
ProE
Early BasoE
Late BasoE
PolyE
OrthoE
CD105
CD71
CD235a

Figure 6

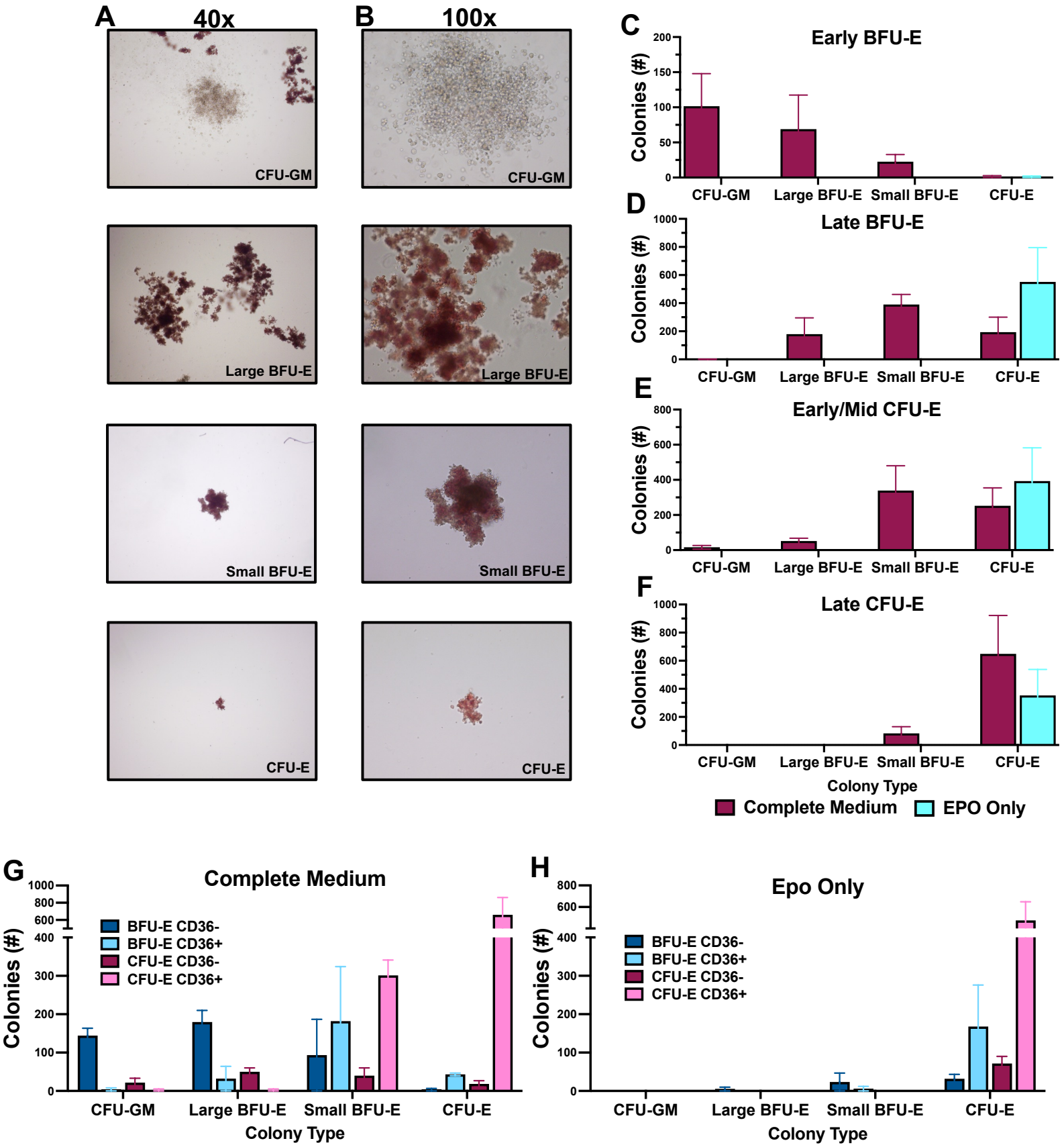
A
40x
B
100x
CFU-GM
CFU-GM
Large BFU-E
Large BFU-E
Small BFU-E
Small BFU-E
CFU-E
CFU-E
C
Early BFU-E
D
Late BFU-E
E
Early/Mid CFU-E
F
Late CFU-E
Colonies (#)
CFU-GM
Large BFU-E
Small BFU-E
CFU-E
Colony Type
Complete Medium
EPO Only
G
Complete Medium
H
Epo Only
BFU-E CD36-
BFU-E CD36+
CFU-E CD36-
CFU-E CD36+

Figure 7

Plots from exp66 D7

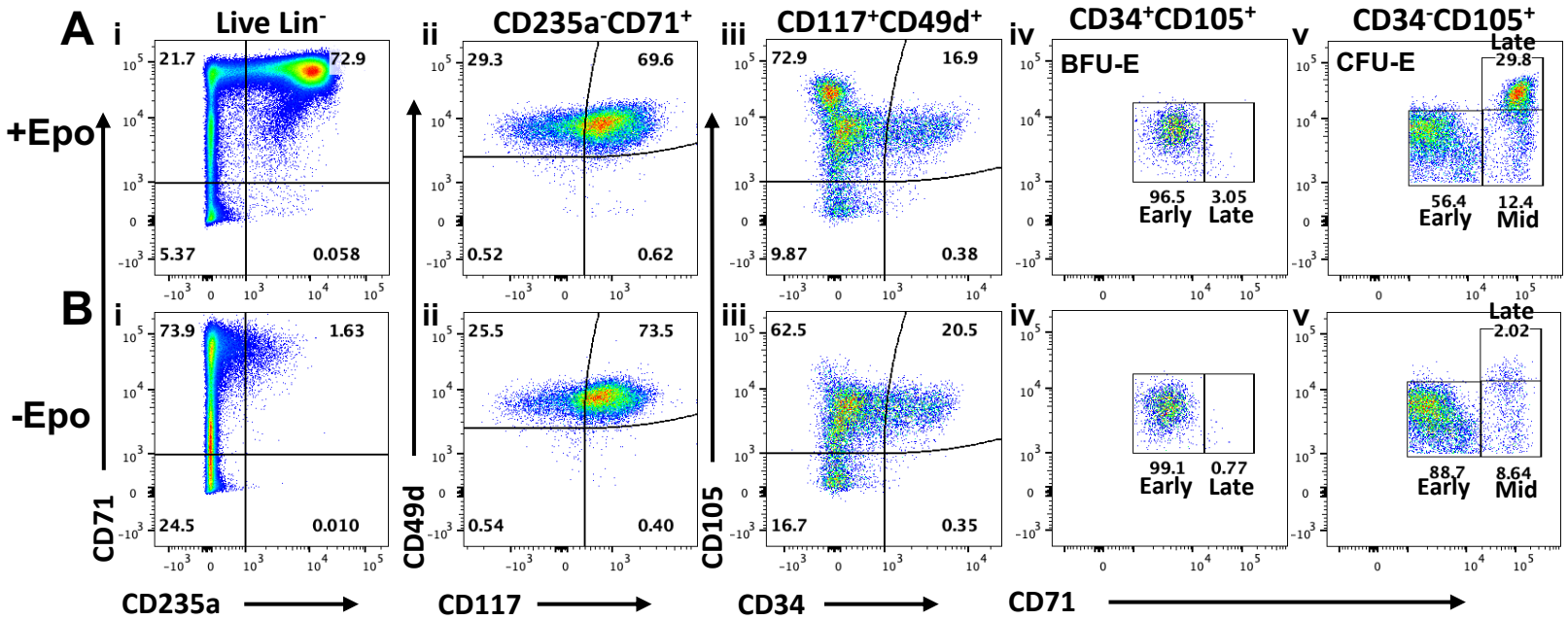


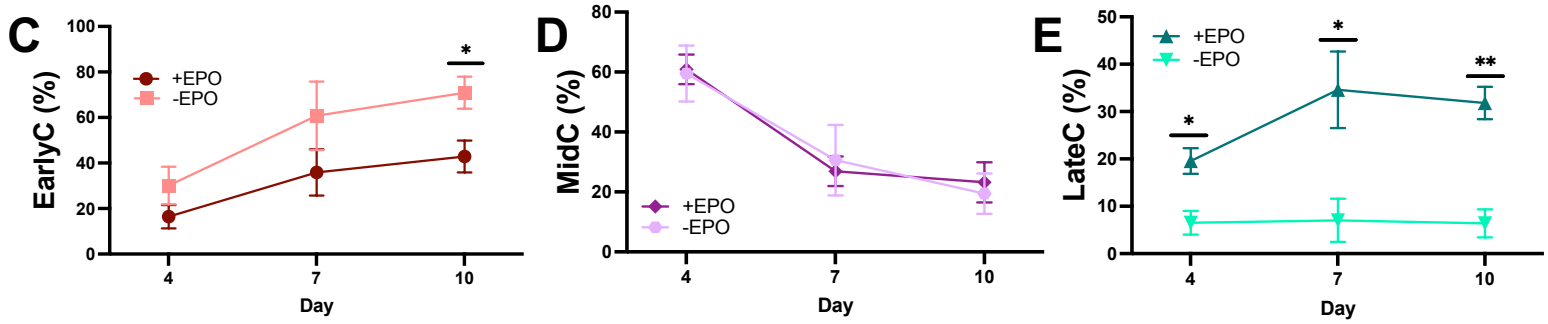


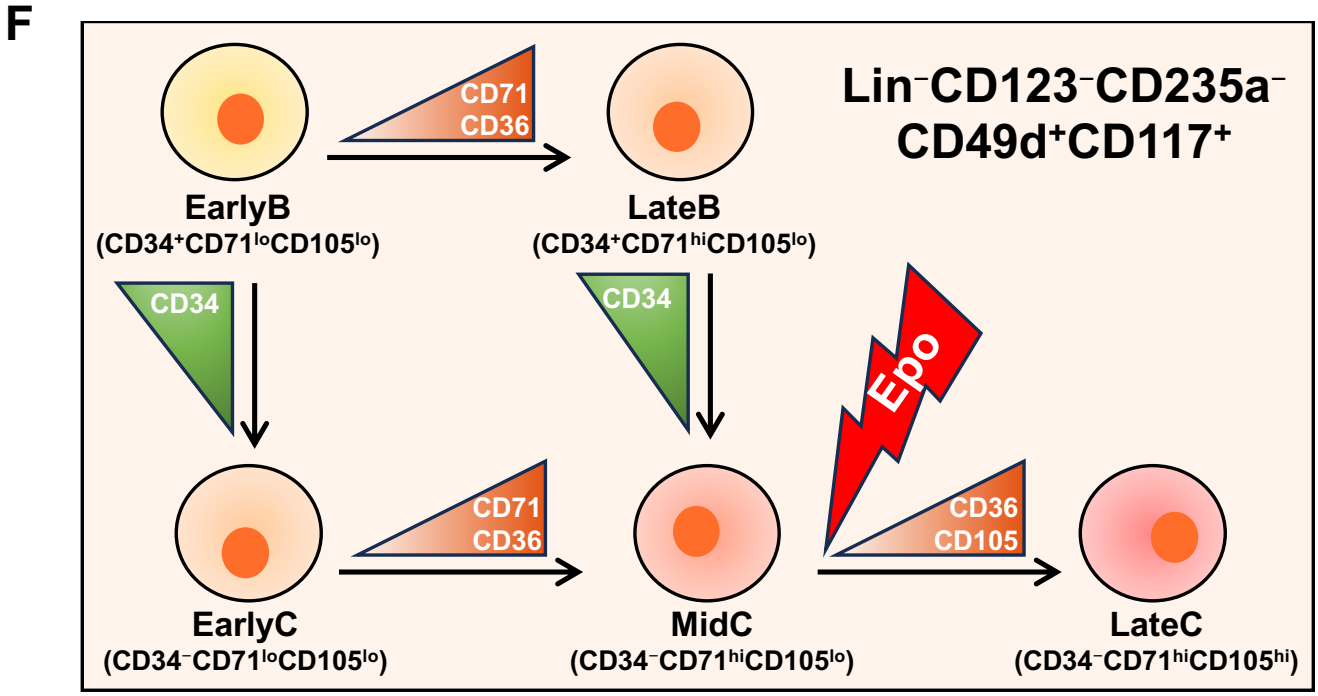

Figure S1

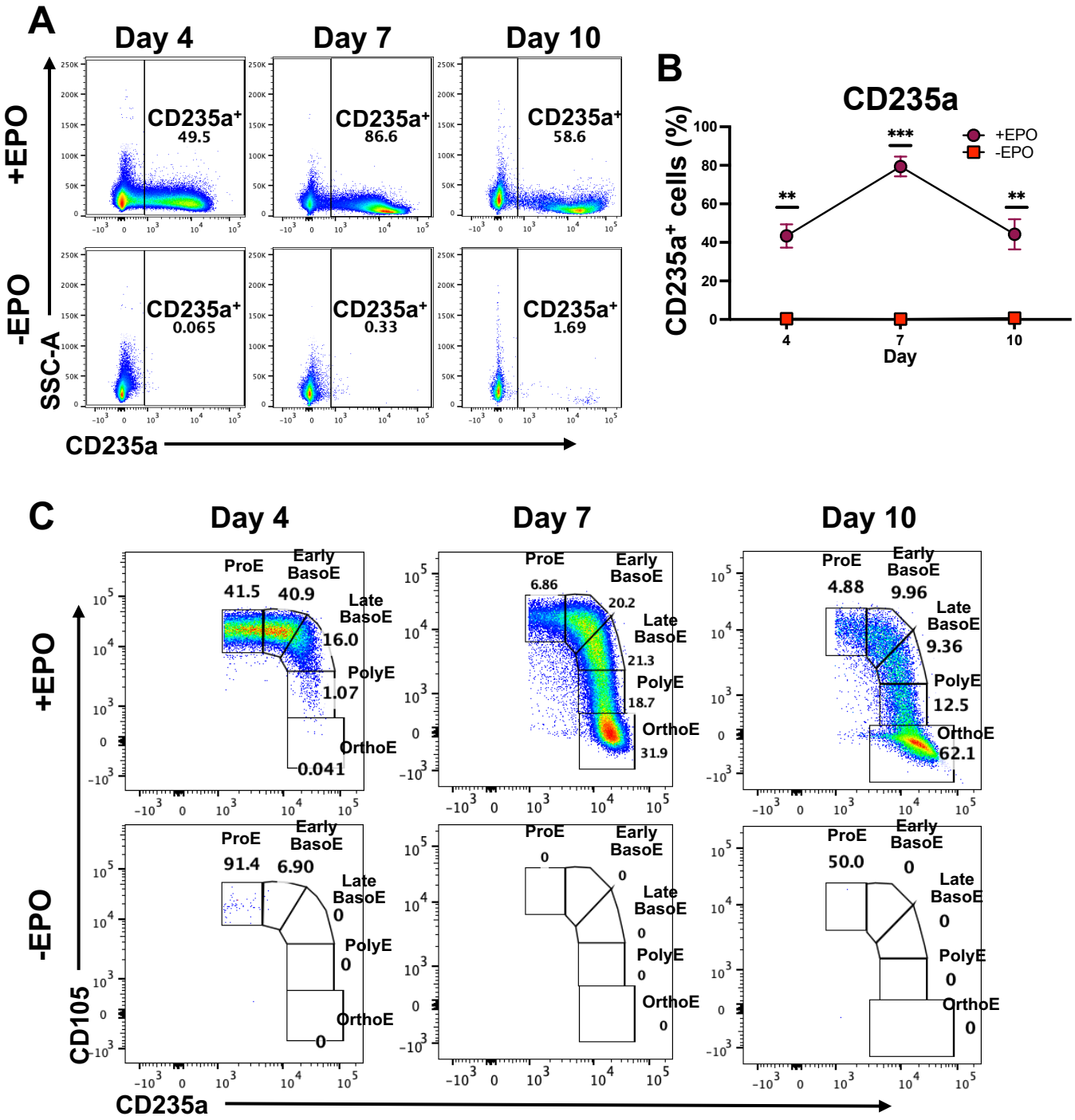
A
Day 4
Day 7
Day 10
+EPO
-EPO
CD235a+
49.5
86.6
58.6
0.065
0.33
1.69
SSC-A
CD235a
B
CD235a
CD235a+ cells (%)
+EPO
-EPO
***
**
**
Day
C
ProE
Early BasoE
Late BasoE
PolyE
OrthoE
41.5
40.9
16.0
1.07
0.041
6.86
20.2
21.3
18.7
31.9
4.88
9.96
9.36
12.5
62.1
91.4
6.90
50.0
CD105

Figure S2

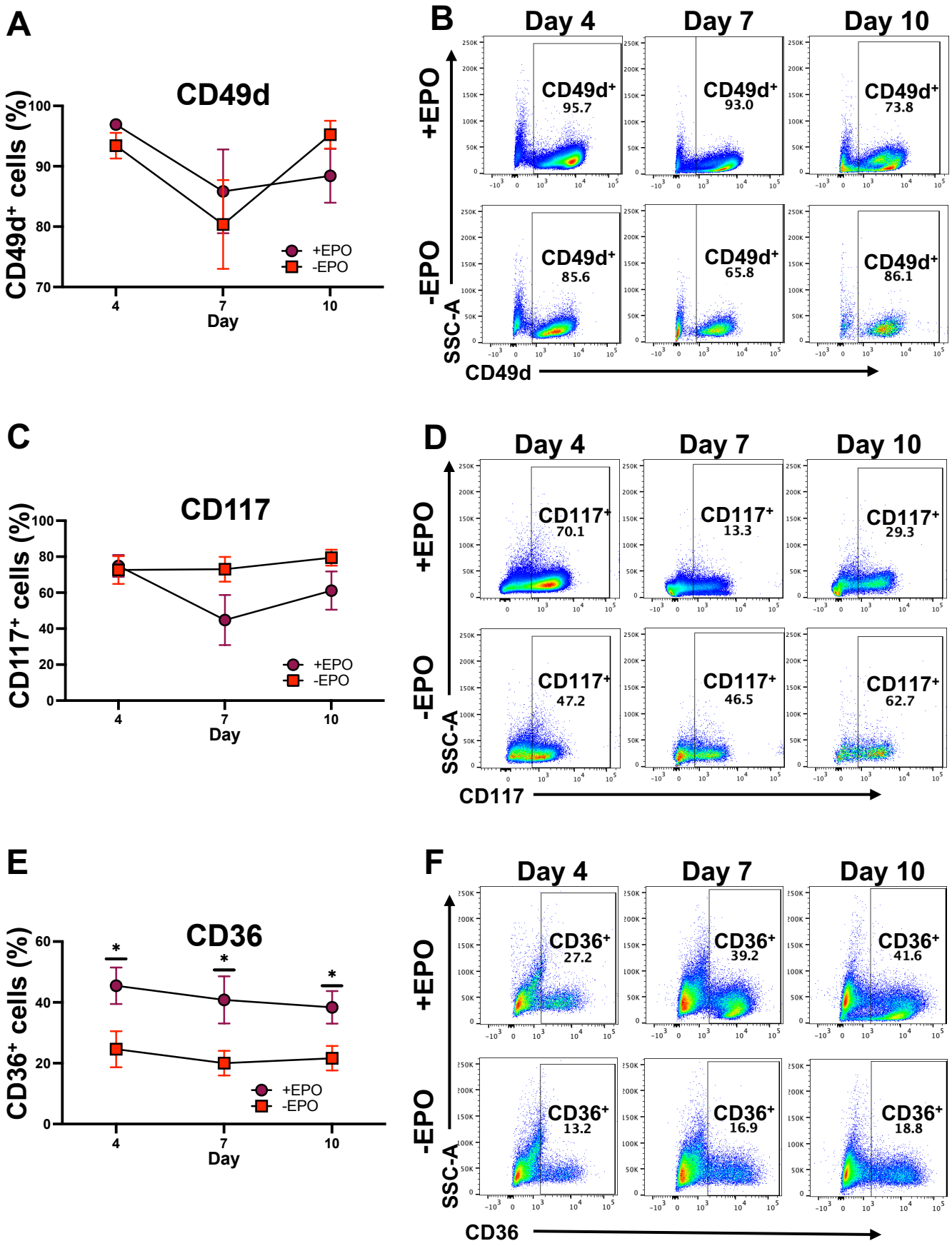
A
CD49d
CD49d+ cells (%)
100
90
80
70
4
7
10
Day
+EPO
-EPO
B
Day 4
Day 7
Day 10
+EPO
-EPO
CD49d+
95.7
CD49d+
93.0
CD49d+
73.8
CD49d+
85.6
CD49d+
65.8
CD49d+
86.1
SSC-A
CD49d
C
CD117
CD117+ cells (%)
100
80
60
40
20
0
4
7
10
Day
+EPO
-EPO
D
Day 4
Day 7
Day 10
+EPO
-EPO
CD117+
70.1
CD117+
13.3
CD117+
29.3
CD117+
47.2
CD117+
46.5
CD117+
62.7
SSC-A
CD117
E
CD36
CD36+ cells (%)
60
40
20
0
*
*
*
4
7
10
Day
+EPO
-EPO
F
Day 4
Day 7
Day 10
+EPO
-EPO
CD36+
27.2
CD36+
39.2
CD36+
41.6
CD36+
13.2
CD36+
16.9
CD36+
18.8
SSC-A
CD36

Figure S3

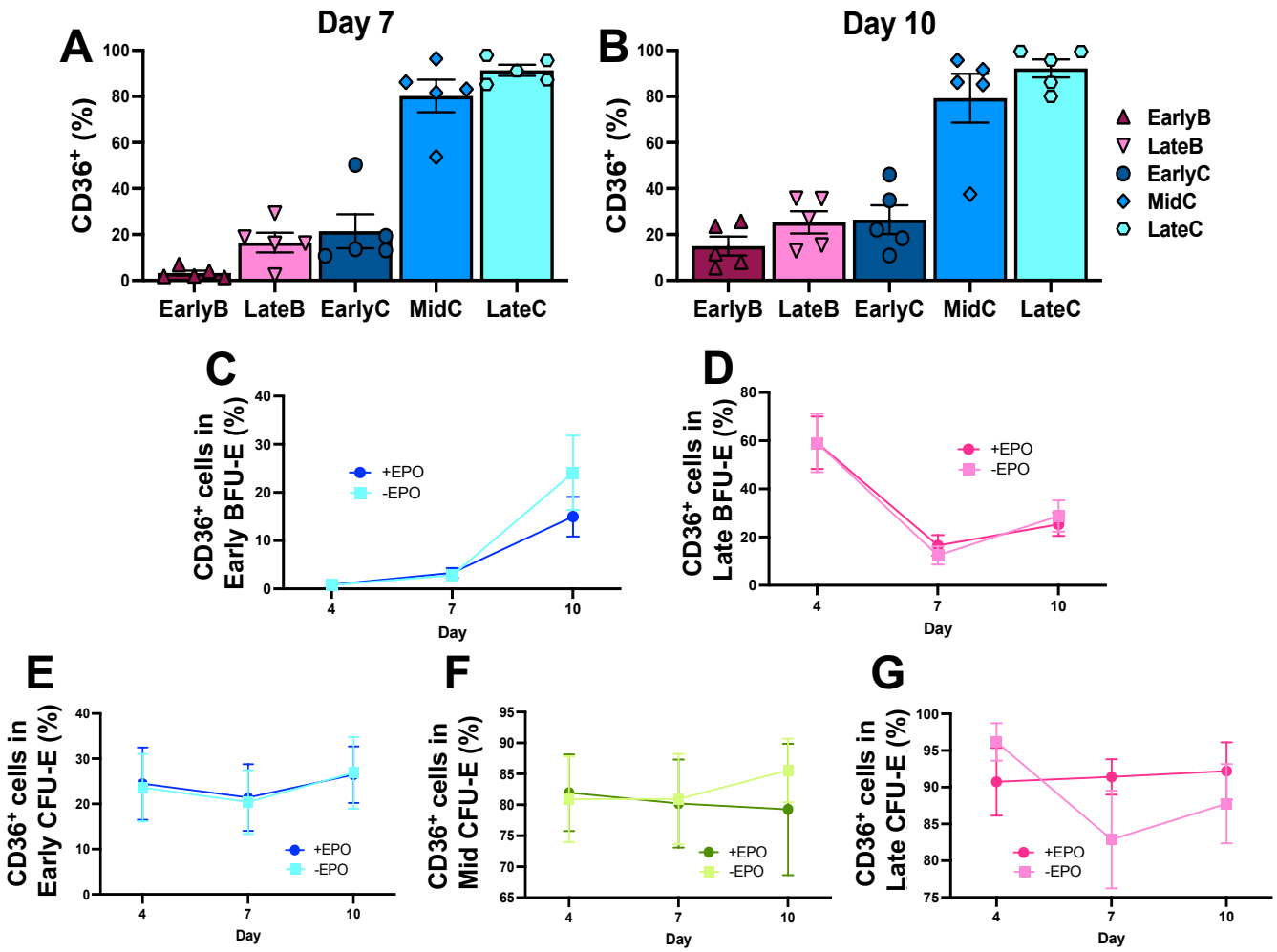
A
Day 7
CD36+ (%)
EarlyB
LateB
EarlyC
MidC
LateC
B
Day 10
EarlyB
LateB
EarlyC
MidC
LateC
C
CD36+ cells in Early BFU-E (%)
+EPO
-EPO
Day
D
CD36+ cells in Late BFU-E (%)
E
CD36+ cells in Early CFU-E (%)
F
CD36+ cells in Mid CFU-E (%)
G
CD36+ cells in Late CFU-E (%)

Figure S4

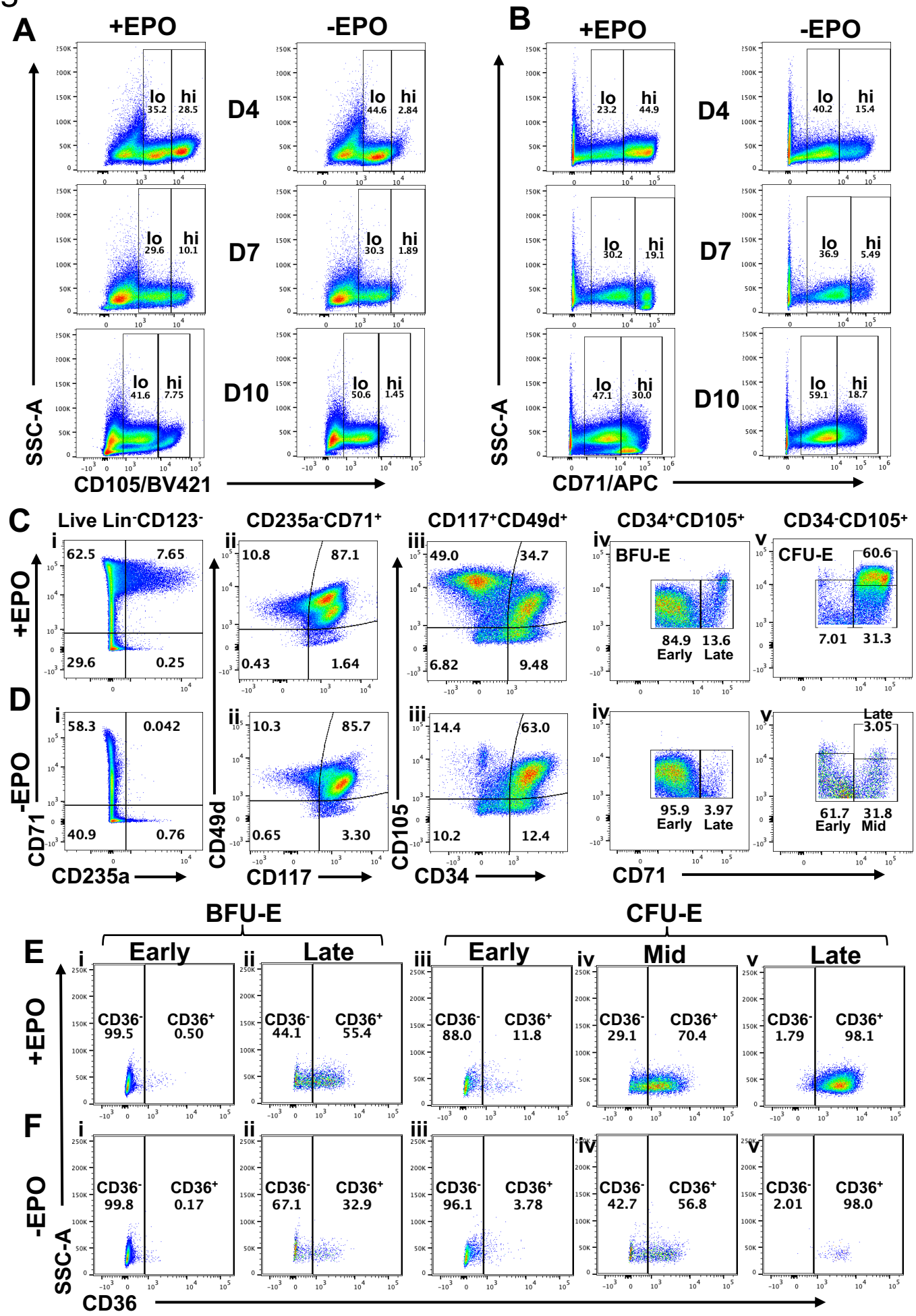
A
+EPO
-EPO
D4
D7
D10
lo 35.2
hi 28.5
lo 44.6
hi 2.84
lo 29.6
hi 10.1
lo 30.3
hi 1.89
lo 41.6
hi 7.75
lo 50.6
hi 1.45
SSC-A
CD105/BV421
B
+EPO
-EPO
D4
D7
D10
lo 23.2
hi 44.9
lo 40.2
hi 15.4
lo 30.2
hi 19.1
lo 36.9
hi 5.49
lo 47.1
hi 30.0
lo 59.1
hi 18.7
SSC-A
CD71/APC
C
Live Lin-CD123-
CD235a-CD71+
CD117+CD49d+
CD34+CD105+
CD34-CD105+
+EPO
i 62.5 7.65 29.6 0.25
ii 10.8 87.1 0.43 1.64
iii 49.0 34.7 6.82 9.48
iv BFU-E 84.9 Early 13.6 Late
v CFU-E 60.6 7.01 31.3
D
-EPO
i 58.3 0.042 40.9 0.76
ii 10.3 85.7 0.65 3.30
iii 14.4 63.0 10.2 12.4
iv 95.9 Early 3.97 Late
v Late 3.05 61.7 Early 31.8 Mid
CD71
CD235a
CD49d
CD117
CD105
CD34
CD71
BFU-E
CFU-E
E
+EPO
i Early CD36- 99.5 CD36+ 0.50
ii Late CD36- 44.1 CD36+ 55.4
iii Early CD36- 88.0 CD36+ 11.8
iv Mid CD36- 29.1 CD36+ 70.4
v Late CD36- 1.79 CD36+ 98.1
F
-EPO
i CD36- 99.8 CD36+ 0.17
ii CD36- 67.1 CD36+ 32.9
iii CD36- 96.1 CD36+ 3.78
iv CD36- 42.7 CD36+ 56.8
v CD36- 2.01 CD36+ 98.0
SSC-A
CD36

# Figure S5

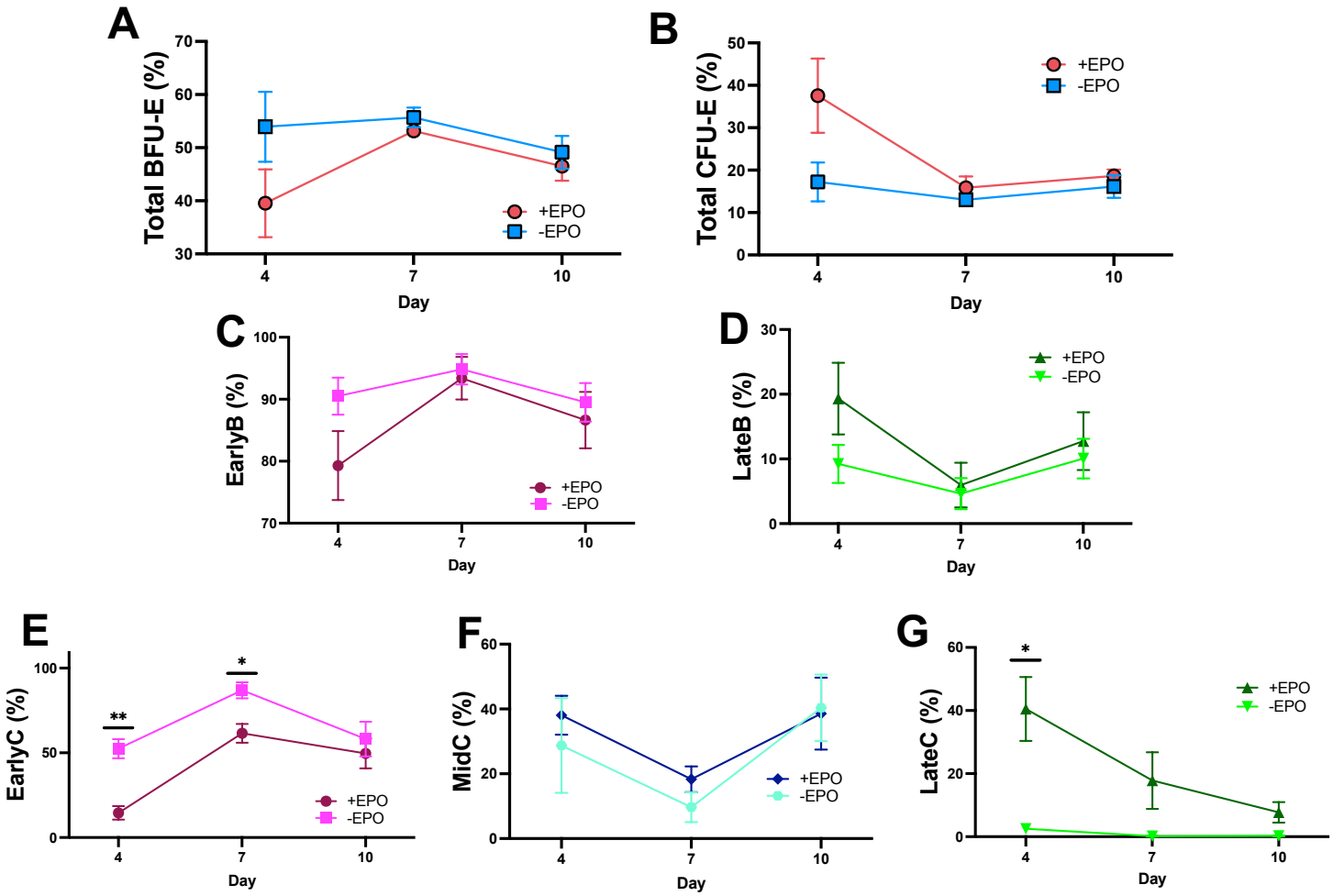
A
Total BFU-E (%)
70
60
50
40
30
4
7
10
Day
+EPO
-EPO
B
Total CFU-E (%)
50
40
30
20
10
0
4
7
10
Day
+EPO
-EPO
C
EarlyB (%)
100
90
80
70
4
7
10
Day
+EPO
-EPO
D
LateB (%)
30
20
10
0
4
7
10
Day
+EPO
-EPO
E
EarlyC (%)
100
50
0
**
*
4
7
10
Day
+EPO
-EPO
F
MidC (%)
60
40
20
0
4
7
10
Day
+EPO
-EPO
G
LateC (%)
60
40
20
0
*
4
7
10
Day
+EPO
-EPO

# Figure S6

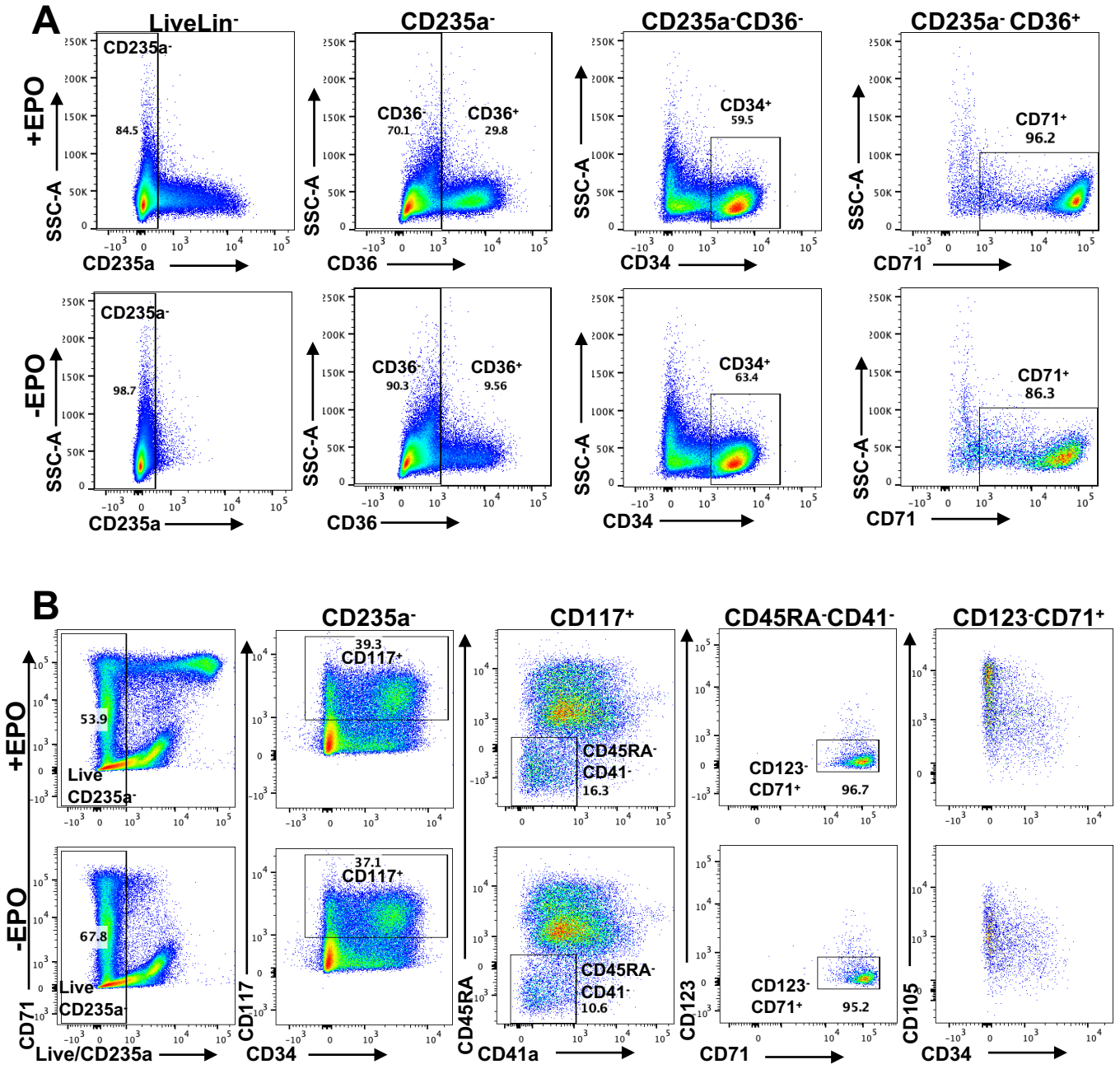
A
LiveLin-
CD235a-
CD235a-CD36-
CD235a- CD36+
+EPO
-EPO
SSC-A
CD235a
CD36
CD34
CD71
84.5
CD36-
70.1
CD36+
29.8
CD34+
59.5
CD71+
96.2
98.7
CD36-
90.3
CD36+
9.56
CD34+
63.4
CD71+
86.3
B
CD235a-
CD117+
CD45RA-CD41-
CD123-CD71+
53.9
Live
CD235a-
39.3
CD117+
CD45RA-
CD41-
16.3
CD123-
CD71+
96.7
67.8
37.1
CD117+
CD45RA-
CD41-
10.6
CD123-
CD71+
95.2
CD71
Live/CD235a
CD117
CD34
CD45RA
CD41a
CD123
CD71
CD105
CD34

Figure S7

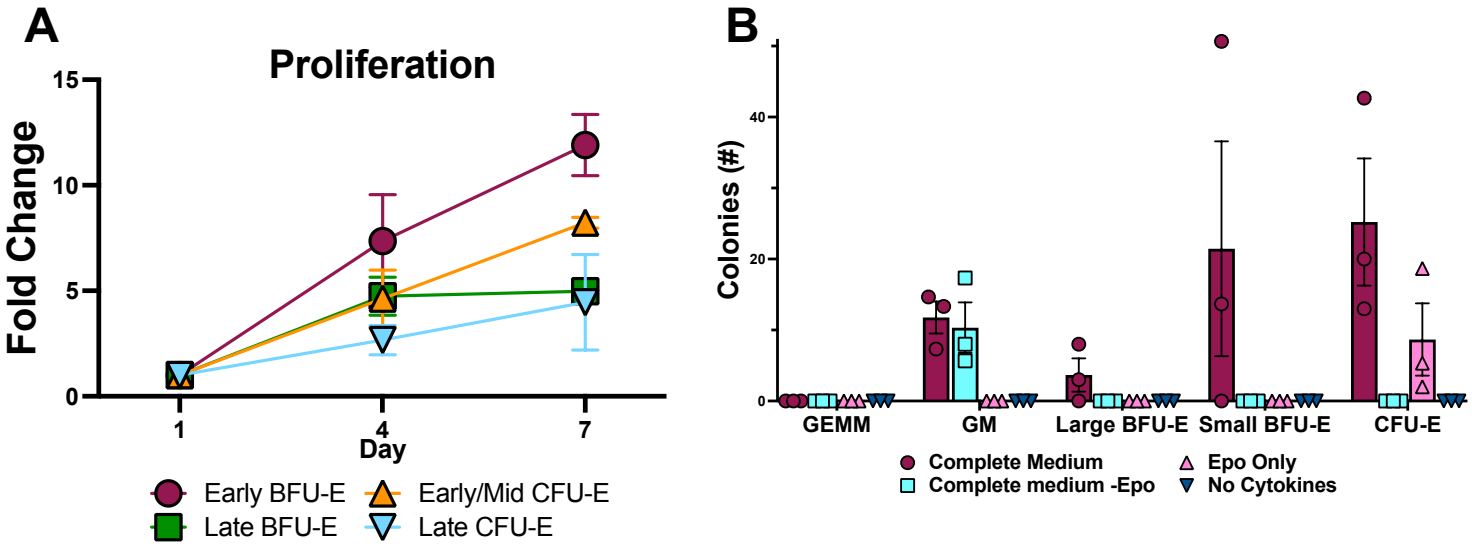
A
Proliferation
Fold Change
15
10
5
0
1
4
7
Day
Early BFU-E
Early/Mid CFU-E
Late BFU-E
Late CFU-E
B
Colonies (#)
40
20
0
GEMM
GM
Large BFU-E
Small BFU-E
CFU-E
Complete Medium
Complete medium -Epo
Epo Only
No Cytokines

# Figure S8

Exp 67

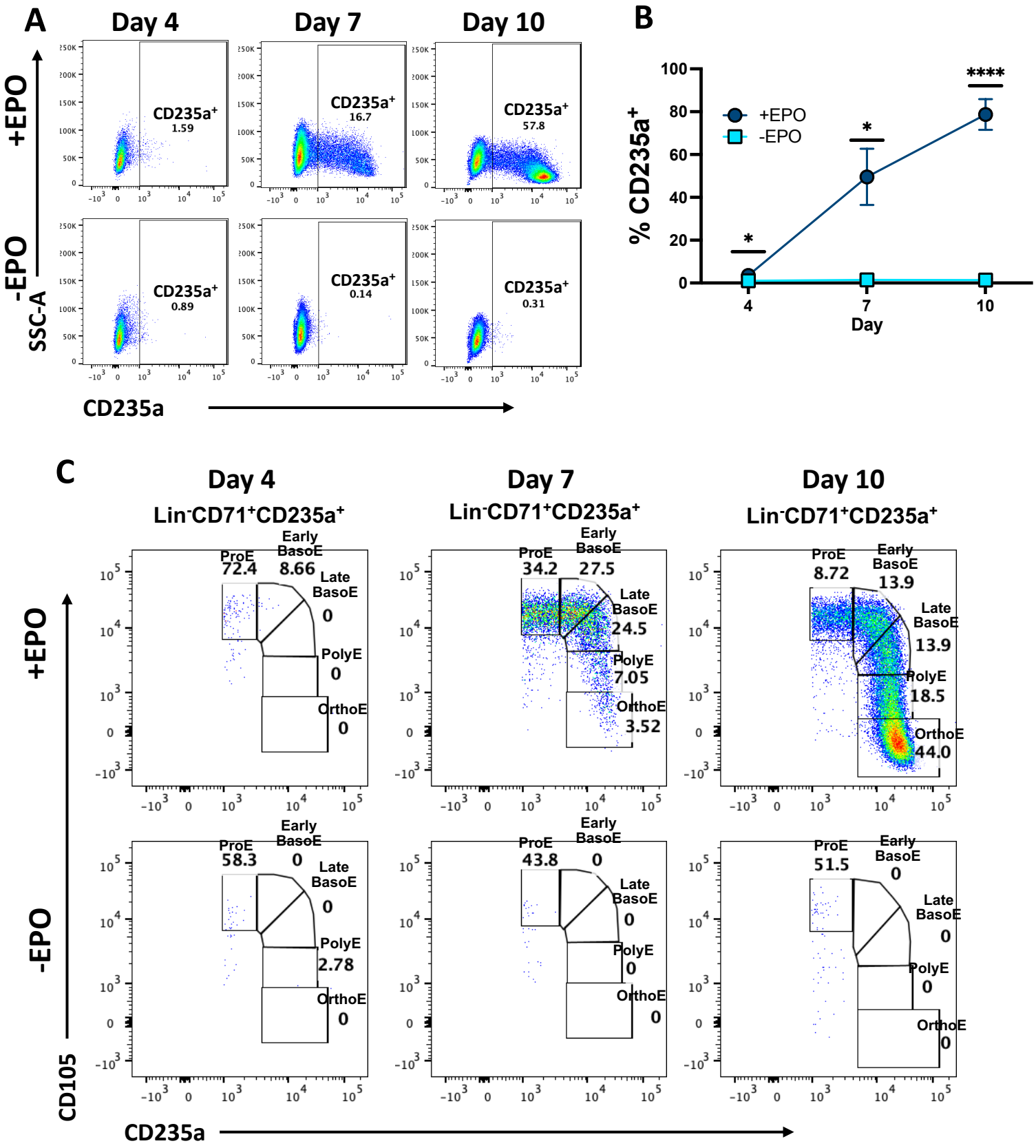

Figure S9

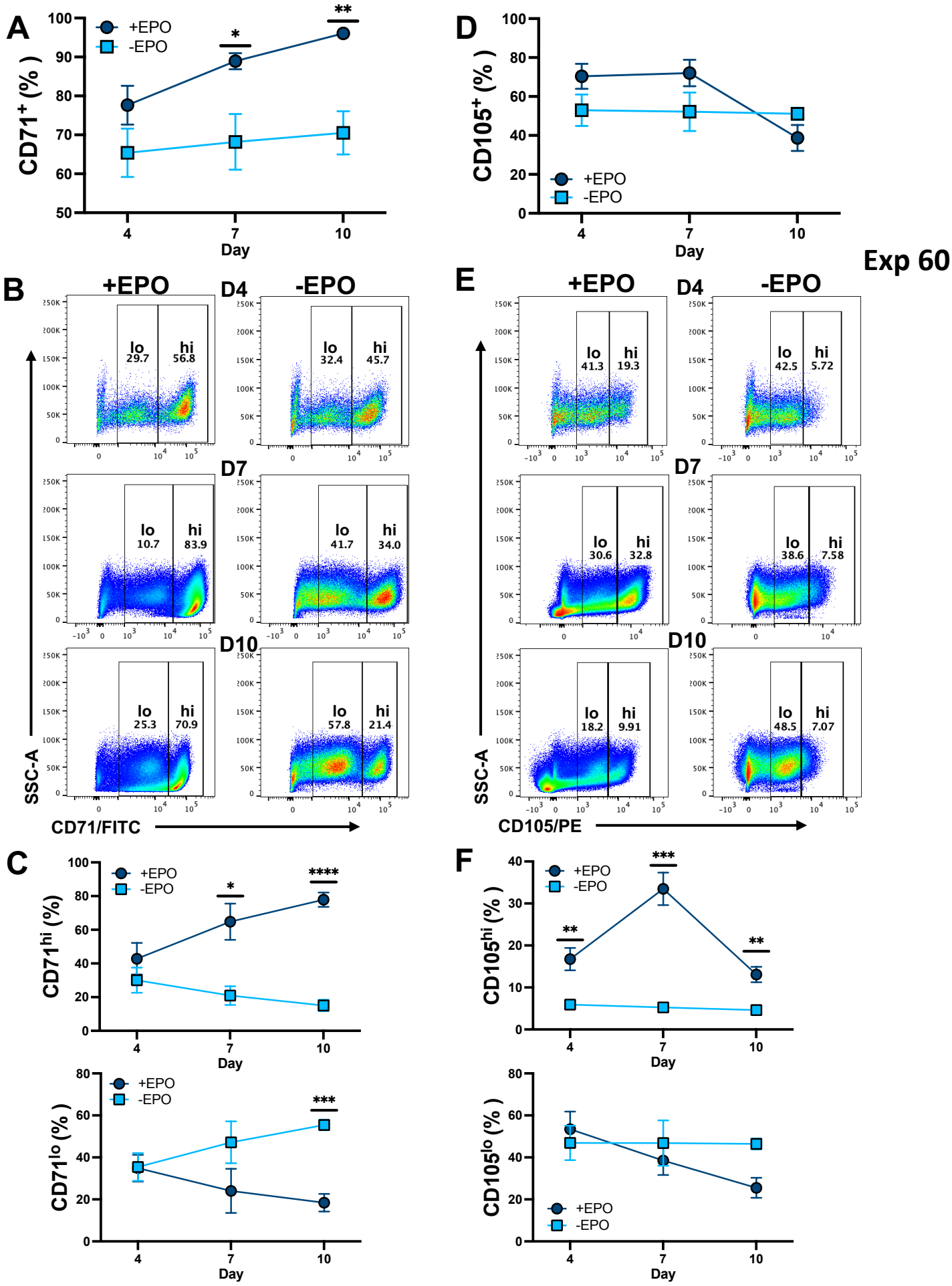
A
+EPO
-EPO
CD71+ (%)
Day
D
CD105+ (%)
Exp 60
B
+EPO
-EPO
D4
D7
D10
lo 29.7
hi 56.8
lo 32.4
hi 45.7
lo 10.7
hi 83.9
lo 41.7
hi 34.0
lo 25.3
hi 70.9
lo 57.8
hi 21.4
SSC-A
CD71/FITC
E
lo 41.3
hi 19.3
lo 42.5
hi 5.72
lo 30.6
hi 32.8
lo 38.6
hi 7.58
lo 18.2
hi 9.91
lo 48.5
hi 7.07
CD105/PE
C
CD71hi (%)
CD71lo (%)
F
CD105hi (%)
CD105lo (%)

Figure S10

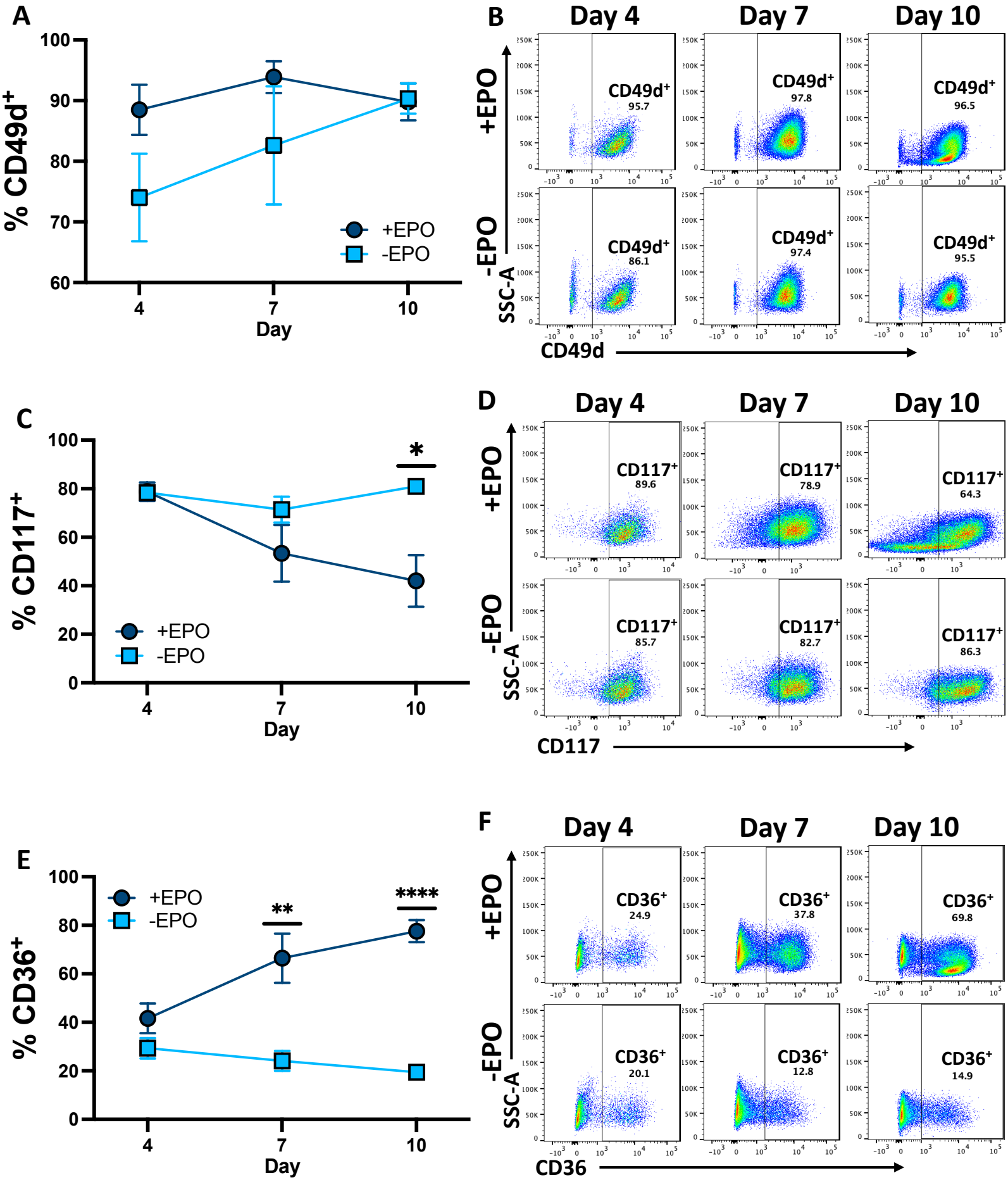


All UCB—plots from exp67

# Figure S11

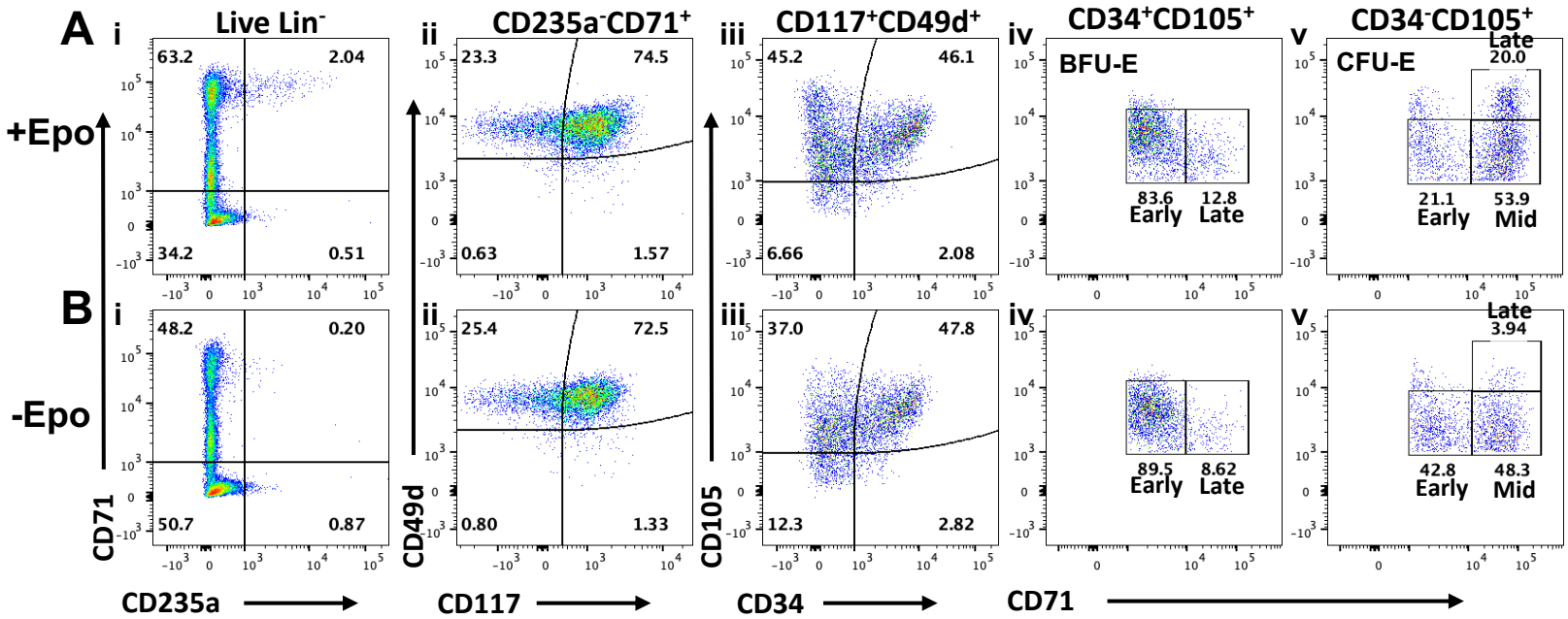
A
B
i
ii
iii
iv
v
Live Lin-
CD235a-CD71+
CD117+CD49d+
CD34+CD105+
CD34-CD105+
+Epo
-Epo
63.2
2.04
34.2
0.51
23.3
74.5
0.63
1.57
45.2
46.1
6.66
2.08
BFU-E
83.6
Early
12.8
Late
CFU-E
Late
20.0
21.1
Early
53.9
Mid
48.2
0.20
50.7
0.87
25.4
72.5
0.80
1.33
37.0
47.8
12.3
2.82
89.5
Early
8.62
Late
Late
3.94
42.8
Early
48.3
Mid
CD71
CD49d
CD105
CD235a
CD117
CD34
CD71

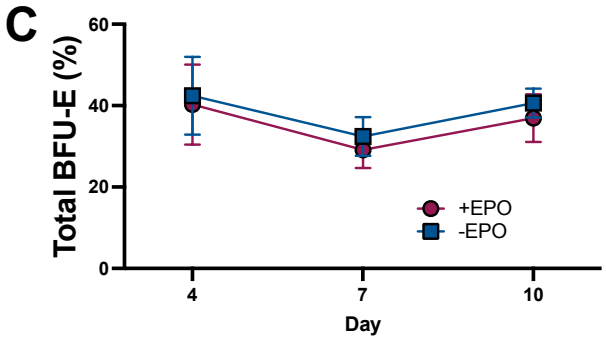
C
Total BFU-E (%)
Day
+EPO
-EPO

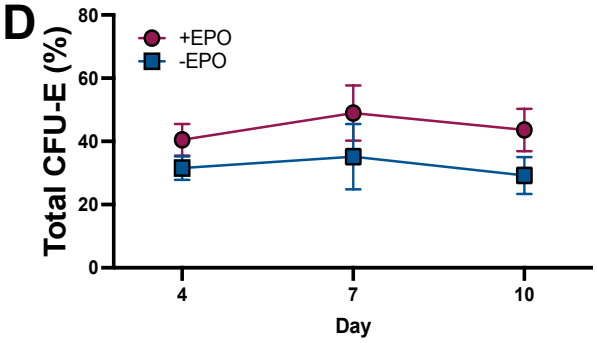
D
Total CFU-E (%)
Day
+EPO
-EPO

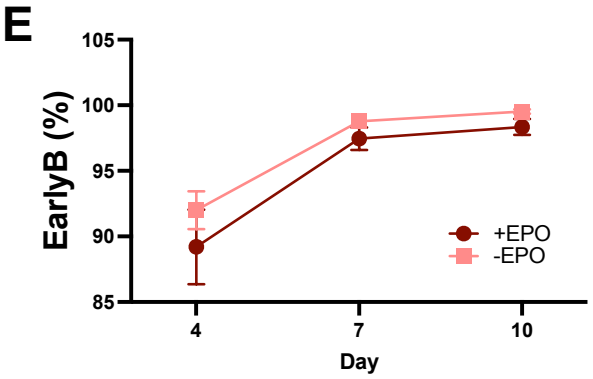
E
EarlyB (%)
Day
+EPO
-EPO

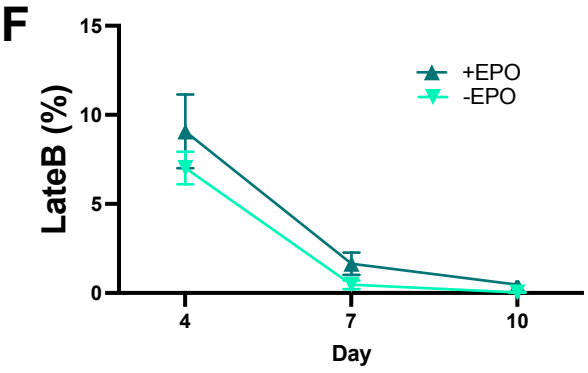
F
LateB (%)
Day
+EPO
-EPO

Figure S12

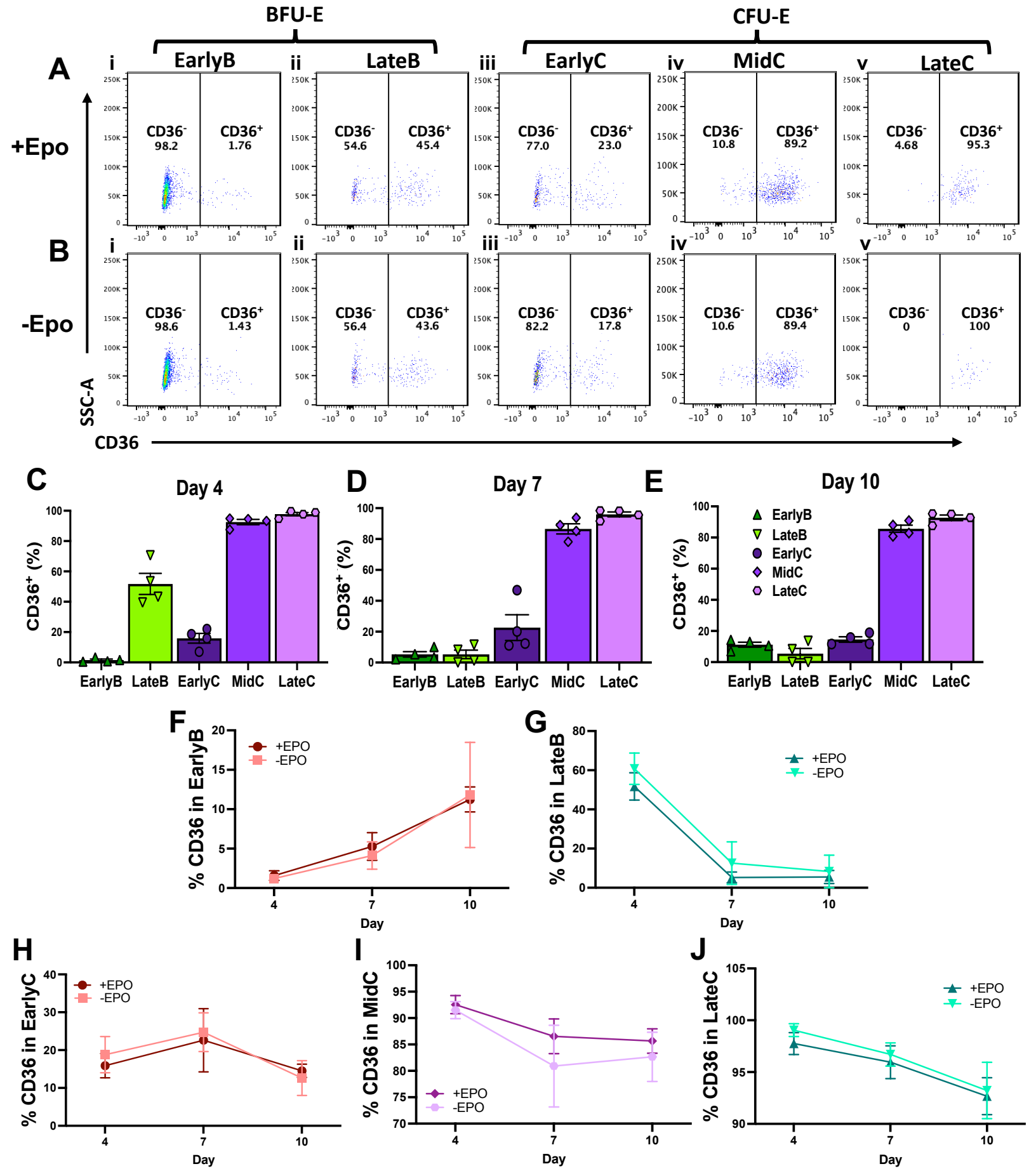
BFU-E
CFU-E
A
B
i EarlyB
ii LateB
iii EarlyC
iv MidC
v LateC
+Epo
-Epo
CD36⁻ 98.2
CD36⁺ 1.76
CD36⁻ 54.6
CD36⁺ 45.4
CD36⁻ 77.0
CD36⁺ 23.0
CD36⁻ 10.8
CD36⁺ 89.2
CD36⁻ 4.68
CD36⁺ 95.3
CD36⁻ 98.6
CD36⁺ 1.43
CD36⁻ 56.4
CD36⁺ 43.6
CD36⁻ 82.2
CD36⁺ 17.8
CD36⁻ 10.6
CD36⁺ 89.4
CD36⁻ 0
CD36⁺ 100
SSC-A
CD36
C Day 4
D Day 7
E Day 10
CD36⁺ (%)
EarlyB
LateB
EarlyC
MidC
LateC
F % CD36 in EarlyB
G % CD36 in LateB
H % CD36 in EarlyC
I % CD36 in MidC
J % CD36 in LateC
+EPO
-EPO
Day

# Figure S13

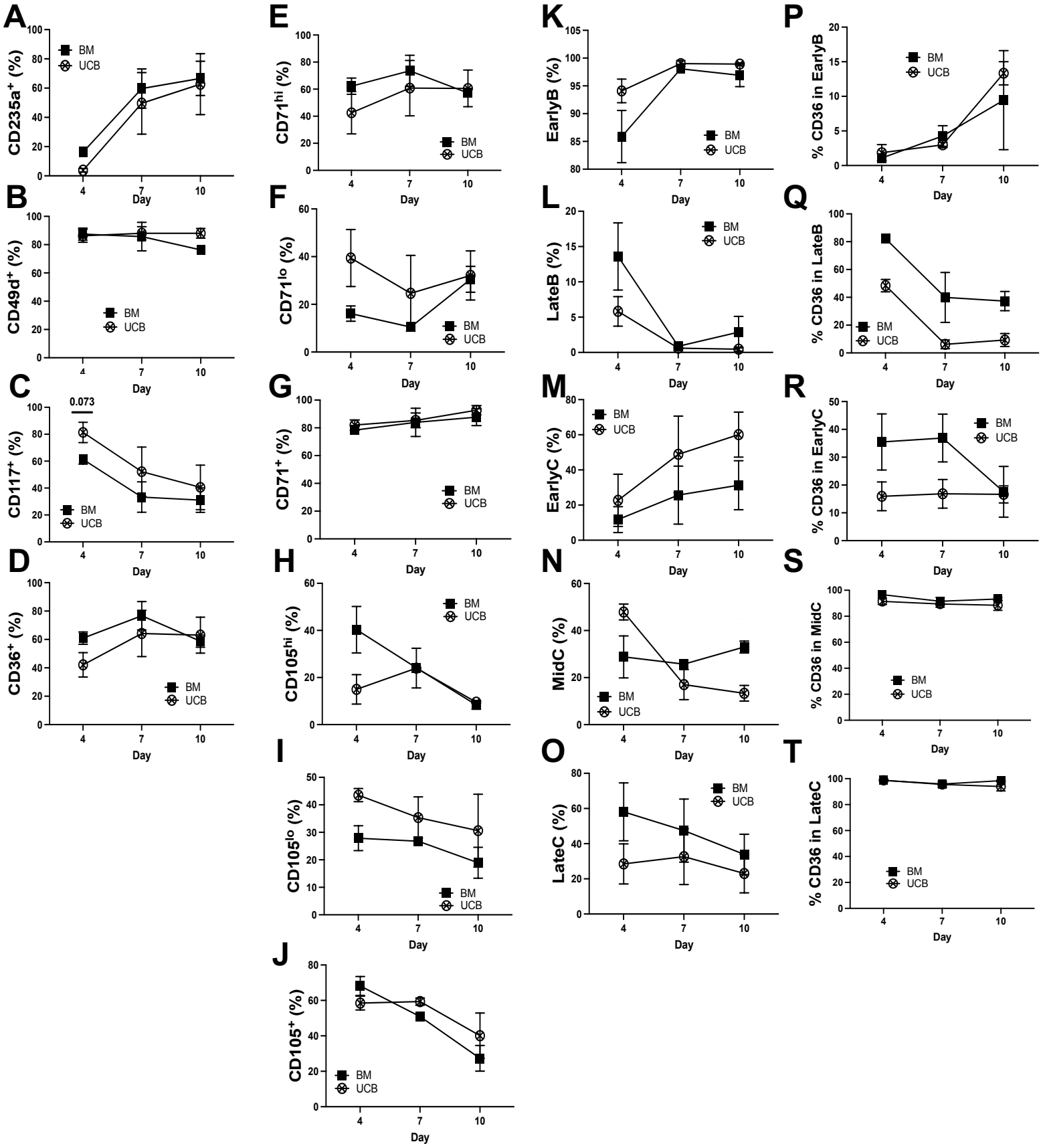
A
CD235a+ (%)
B
CD49d+ (%)
C
CD117+ (%)
0.073
D
CD36+ (%)
E
CD71hi (%)
F
CD71lo (%)
G
CD71+ (%)
H
CD105hi (%)
I
CD105lo (%)
J
CD105+ (%)
K
EarlyB (%)
L
LateB (%)
M
EarlyC (%)
N
MidC (%)
O
LateC (%)
P
% CD36 in EarlyB
Q
% CD36 in LateB
R
% CD36 in EarlyC
S
% CD36 in MidC
T
% CD36 in LateC
BM
UCB
Day

Figure S14

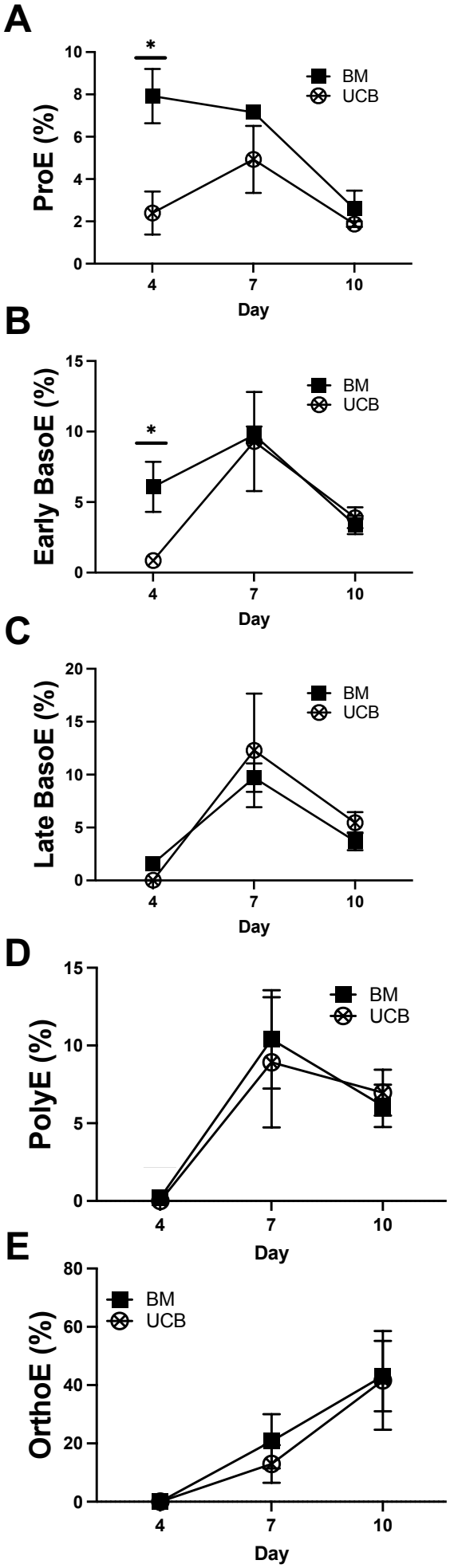
A
ProE (%)
Day
BM
UCB
*
B
Early BasoE (%)
Day
BM
UCB
*
C
Late BasoE (%)
Day
BM
UCB
D
PolyE (%)
Day
BM
UCB
E
OrthoE (%)
Day
BM
UCB

Supplemental Table 1

**Table S1.** Immunophenotypes of EE progenitor populations.

| **Population** | **Phenotype** |
|---|---|
| Early BFU-E | $Lin^{-}CD123^{-}CD235a^{-}CD49d^{+}CD117^{+}CD34^{+}CD71^{lo}CD105^{lo}$ |
| Late BFU-E | $Lin^{-}CD123^{-}CD235a^{-}CD49d^{+}CD117^{+}CD34^{+}CD71^{hi}CD105^{lo}$ |
| Early CFU-E | $Lin^{-}CD123^{-}CD235a^{-}CD49d^{+}CD117^{+}CD34^{-}CD71^{lo}CD105^{lo}$ |
| Mid CFU-E | $Lin^{-}CD123^{-}CD235a^{-}CD49d^{+}CD117^{+}CD34^{-}CD71^{hi}CD105^{lo}$ |
| Late CFU-E | $Lin^{-}CD123^{-}CD235a^{-}CD49d^{+}CD117^{+}CD34^{-}CD71^{hi}CD105^{hi}$ |
| Lineage (Lin) | CD3, CD10, CD11b, CD19, CD41a |

Supplemental Table 2

**Table S2.** Antibody panels used for flow cytometry analysis.

| **Panel 1 (Main)** | | | | |
|---|---|---|---|---|
| Marker | Fluorophore | Clone | Manufacturer | Catalog # |
| 7AAD | 7AAD | | Biolegend | 420404 |
| CD3-PerCP-Cy5.5 | PerCP-Cy5.5 | UCHT1 | Biolegend | 300430 |
| CD10-PerCP-Cy5.5 | PerCP-Cy5.5 | H110a | Biolegend | 312216 |
| CD11b-PerCP-Cy5.5 | PerCP-Cy5.5 | CBRM1/5 | Biolegend | 301418 |
| CD19-PerCP-Cy5.5 | PerCP-Cy5.5 | HIB19 | Biolegend | 302230 |
| CD41a-PerCP-Cy5.5 | PerCP-Cy5.5 | HIP8 | Biolegend | 303720 |
| CD123-PerCP-Cy5.5 | PerCP-Cy5.5 | 6H6 | Biolegend | 306016 |
| CD34-APC-Cy7 | APC-Cy7 | 581 | Biolegend | 343514 |
| CD49d-APC | APC | 9F10 | Biolegend | 304307 |
| CD117-BV510 | BV510 | 104D2 | Biolegend | 313220 |
| CD105-PE | PE | SN6h | Biolegend | 800504 |
| CD71-FITC | FITC | CY1G4 | Biolegend | 334104 |
| CD36-BV421 | BV421 | 5-271 | Biolegend | 336230 |
| CD235a-PE-Cy7 | PE-Cy7 | HIR2 | BD Biosciences | 563666 |
| | | | | |
| **Panel 2 (Alternative)** | | | | |
| Marker | Fluorophore | Clone | Manufacturer | Catalog # |
| 7AAD | 7AAD | | Biolegend | 420404 |
| CD3-PerCP-Cy5.5 | PerCP-Cy5.5 | UCHT1 | Biolegend | 300430 |
| CD10-PerCP-Cy5.5 | PerCP-Cy5.5 | H110a | Biolegend | 312216 |
| CD11b-PerCP-Cy5.5 | PerCP-Cy5.5 | CBRM1/5 | Biolegend | 301418 |
| CD19-PerCP-Cy5.5 | PerCP-Cy5.5 | HIB19 | Biolegend | 302230 |
| CD41a-PerCP-Cy5.5 | PerCP-Cy5.5 | HIP8 | Biolegend | 303720 |
| CD123-PerCP-Cy5.5 | PerCP-Cy5.5 | 6H6 | Biolegend | 306016 |
| CD34-APC-Cy7 | APC-Cy7 | 581 | Biolegend | 343514 |
| CD117-BV510 | BV510 | 104D2 | Biolegend | 313220 |
| CD235a-PE-Cy7 | PE-Cy7 | HIR2 | BD Biosciences | 563666 |
| CD49d-PE | PE | 9F10 | Biolegend | 304304 |
| CD105-BV421 | BV421 | SN6h | Biolegend | 800510 |
| CD71-APC | APC | CY1G4 | Biolegend | 334108 |
| CD36-FITC | FITC | 5-271 | Biolegend | 336204 |
| | | | | |
| Antibody used in some experiments in lieu of CD235a-PE-Cy7 | | | | |
| Marker | Fluorophore | Clone | Manufacturer | Catalog # |
| CD235a-PerCP-Cy5.5 | PerCP-Cy5.5 | HIR2 | Biolegend | 306610 |